J of Nuclear Medicine Technology, first published online October 5, 2020 as doi:10.2967/jnmt.120.246157

Title

Texture feature comparison between step-and-shoot and continuous bed motion in ^{18}F-fluorodeoxyglucose positron emission tomography

Short Title

Effect of scan types on texture analysis

Authors name and affiliations

Shozo Yamashita[1], Koichi Okuda[2], Tetsu Nakaichi[1], Haruki Yamamoto[1], and Kunihiko Yokoyama[3]

1. Division of Radiology, Public Central Hospital of Matto Ishikawa, 3-8 Kuramitsu, Hakusan, Ishikawa 924-8588, Japan

2. Department of Physics, Kanazawa Medical University, Uchinada, Kahoku, Japan

3. PET Imaging Center, Public Central Hospital of Matto Ishikawa, 3-8 Kuramitsu, Hakusan, Ishikawa 924-8588, Japan

Corresponding author

Shozo Yamashita (First author)
E-mail : y.shozo57@gmail.com
TEL : +81-76-275-2222, FAX : +81-76-274-5974

Word Counts：5797

Abstract

Objective: To investigate the differences in texture features between step-and-shoot (SS) and continuous bed motion (CBM) imaging in phantom and clinical studies.

Methods: A NEMA body phantom was filled with ^{18}F-fluorodeoxyglucose solution at a sphere-to-background ratio of 4:1. SS and CBM were performed using the same acquisition duration and the data were reconstructed using 3-D ordered subset expectation maximization with time-of-flight algorithms. Texture features were extracted using the software LIFEx. A volume of interest was delineated on the 22-, 28-, and 37-mm spheres with a threshold of 42% of the maximum standardized uptake value. The voxel intensities were discretized using two resampling methods, namely, a fixed bin size and a fixed bin number discretization. The discrete resampling values were set to 64 and 128. A total of 31 texture features were calculated with gray-level co-occurrence matrix (GLCM), gray-level run length matrix, neighborhood gray-level different matrix, and gray-level zone length matrix. The texture features of the SS and CBM images were compared for all settings using the paired t-test and the coefficient of variation (CV). In a clinical study, a total of 27 lesions from 20 patients were examined using the same acquisition and image processing that was performed during the phantom study. The % difference (%Diff) and correlation between the texture features from SS and CBM images were calculated to evaluate the agreement of the two scanning techniques.

Results: In the phantom study, the 11 features exhibited no significant difference between SS and CBM images

and CV of ≤10% depending on resampling conditions, whereas entropy and dissimilarity from GLCM fulfilled the criteria for all settings. In the clinical study, the entropy and dissimilarity from GLCM exhibited low %Diff and excellent correlation in all resampling conditions. %Diff of the entropy was lower than that of dissimilarity.

Conclusions: The magnitude in differences between texture features of SS and CBM images were different depending on types of features. Because entropy for GLCM exhibits minimal differences between SS and CBM images irrespective of resampling conditions, it may be the optimal feature to reduce the differences between the two scanning techniques.

Keywords: step-and-shoot, continuous bed motion, texture feature, resampling, sphere size

Introduction

Standardized uptake value (SUV) is generally applied for semi-quantitative evaluation of positron emission tomography (PET) images in clinical practice. Specifically, maximum SUV (SUVmax) and mean SUV (SUVmean) are the most popular features to provide information about the metabolic activity in tumors. Further, metabolic tumor volume (MTV) and total lesion glycolysis, which is defined as MTV × SUVmean, have been proposed to measure the tumor volume and metabolic activity, respectively *(1)*. These parameters, however, cannot measure the intratumoral spatial distribution in tumors, because SUVmax is derived from the concentration in a single voxel, and SUVmean is the average value of all voxels within a volume of interest (VOI).

In recent years, texture analysis has been used to evaluate the intratumoral heterogeneity in oncologic PET imaging. Texture analysis can potentially provide beneficial information to predict therapy response and assess prognosis for various tumors *(2–8)*. However, texture features are greatly influenced by various technical factors, such as reconstruction settings, acquisition modes (2-D and 3-D), segmentation, resampling, and respiratory motion *(9-14)*. Although texture features are sensitive to these factors, the difference between texture features of step-and-shoot (SS) and continuous bed motion (CBM) images has yet to be investigated. When comparing the image quality of SS and CBM images we found that in the visual analysis, the CBM images showed slightly higher noises than the SS images, and in the quantitative analysis, the CBM images

exhibited slightly lesser uniformity and higher variability in SUV analysis *(15)*. Since texture analysis considerably depends on the image quality *(10, 13)*, it could be sensitive to the subtle differences in image quality between the two scanning techniques. Therefore, we need to investigate whether the SS and CBM techniques produce comparable results when performing texture analysis. The objective of this study, therefore, are (1) to investigate the differences between the texture features of SS and CBM images, and (2) to find features for reduction of the differences between the two scanning techniques by using phantom and clinical studies.

Materials and methods

This study was conducted using the data of a previous research study *(15)*.

Phantom study

Phantom preparation

A NEMA International Electrotechnical Commission body phantom (Data Spectrum Corp., Hillsborough, NC, USA) with spherical objects of diameters 10 mm, 13 mm, 17 mm, 22 mm, 28 mm, and 37 mm was used. The phantom was filled with a ^{18}F-fluorodeoxyglucose (^{18}F-FDG) solution at a sphere-to-background radioactivity ratio of 4:1. The hot spheres and background radioactivity were set to 13.2 kBq/mL and 3.3 kBq/mL,

respectively. The background radioactivity simulated a normal soft-tissue uptake, especially in the mediastinum or abdomen of patients who received injected dose of our institution.

Data acquisition and image reconstruction

All PET/CT data were acquired using a Biograph mCT Flow 20-4R (Siemens Medical Solutions USA, Inc., Knoxville, USA). The scanner comprises four detector rings of diameter 842 mm with 48 detector blocks in each ring, covering an axial field of view (FOV) of 216 mm and a transaxial FOV of 700 mm. The detector comprises an array of 32,448 lutetium oxyorthosilicate crystals of the dimension $4 \times 4 \times 20$ mm^3. The coincidence timing window and the time-of-flight (TOF) time resolution were 4.1 ns and 540 ps, respectively.

The phantom was scanned using the SS and the CBM techniques, with a respective phantom for each experiment. Images acquired using the SS technique was done over eight bed positions that is typical during clinical imaging. Hot spheres were placed at the center of the axial FOV, which corresponds to the center of the overlap region between bed positions 4 and 5. The acquisition time was set as 1.5 min/bed. The CBM protocol matched the axial FOV of the SS technique. The table speed was set at 1.5 mm/s to be consistent with the total scan time of the SS technique; the CBM acquisition time was 12 min 13 s. Considering the statistical variability of PET images, each image acquisition was performed 5 times.

The PET data were reconstructed using 3-D ordered subset expectation maximization and TOF algorithms with iteration-subset combinations of 3–21. In addition, a full width at half-maximum Gaussian filter of 5 mm was used. The reconstructed voxel size was 4.0 × 4.0 × 3.0 mm^3, and the matrix size was 200 × 200. All PET images were converted into SUV units normalized by the patient body weight using the following formula: tissue radioactivity (Bq/mL)/[injected radioactivity (Bq)/body weight (g)]. Further, attenuation correction using the CT data was performed with the following scanning parameters: tube voltage–120 kV, quality reference –40 mAs, rotation time–0.5 s, pitch–1.0, slice thickness–3.0 mm, transaxial FOV–780 mm, and matrix size–512 × 512. The CT images were reconstructed using the sinogram-affirmed iterative reconstruction algorithm.

Texture analysis

The texture features were extracted using the software LIFEx ver.4.00 *(16)*. The VOI was delineated on the three largest spheres of 22–37 mm with a threshold of 42% of SUVmax, which was selected based on previous work *(17)*. Analyzing the spheres of equal to and less than 17 mm was not possible due to insufficient number of voxels because LIFEx calculates the features only for VOI of at least 64 voxels. Moreover, delineations were performed by two observers to examine inter-observer differences. The original voxel intensities were discretized using two resampling methods, namely, a fixed bin size (FBS) discretization with scale bounds between 0 and 20 SUV, and

a fixed bin number (FBN) discretization with scale bounds between minimum and maximum SUV. The discrete values were set at 64 and 128 for these methods, whereas the bin widths of the FBS discretization were 0.31 and 0.16 SUV, respectively. A total of 31 texture features were calculated including parameters from gray-level co-occurrence matrix (GLCM), gray-level run length matrix (GLRLM), neighborhood gray-level different matrix (NGLDM), and gray-level zone length matrix (GLZLM). All the features are presented in Table 1. The GLCM was calculated using a distance equal to 1. Detailed descriptions of texture calculations can be found at http://www.lifexsoft.org.

The coefficient of variation (CV) was calculated for each sphere size. The CV was calculated using the ratio of standard deviation (SD) to the average values using a total of 10 data sets (5 data sets per observer).

To search the texture features for the reduction in the differences between the SS and CBM images in the uniform phantom, we defined the criteria A: (1) No significant differences in texture features between SS and CBM images confirmed in all sphere sizes. (2) SS and CBM images had CV of ≤10% for all sphere sizes.

Clinical study

Patients

Whole-body ^{18}F-FDG PET/CT images acquired by SS and CBM were obtained in a clinical setting. A total of 27 lesions from 20 patients (male, 10; female, 10; average age, 69.1 ± 11.9 years, average body mass index, 23.4 ± 3.7 kg/m^2) were retrospectively examined; these lesions included 1 in the salivary glands, 4 in the thyroid, 6 in the lung, 1 in the breast tissue, 2 in the esophagus, 1 in the liver, 2 in the pancreas, 1 in the adrenal, 1 in the lumbar spine, 5 in the lymph nodes and 3 in the lower abdomen. All subjects were asked to fast for at least 5 h before imaging. ^{18}F-FDG was intravenously injected with radioactivity of 4.4 MBq/kg (maximum dose, 330 MBq), and PET images were acquired 60 min after tracer injection. Both PET and CT images were acquired during free breathing. A subset of six patients with eight lesions was imaged using the SS technique, followed immediately by the CBM technique (SS→CBM). The remaining 14 patients with 19 lesions were scanned in the reverse order (CBM→SS). The image acquisition and reconstruction protocols were the same as those described in the phantom study. This study was approved by the ethics committee of our institution. Written informed consent was obtained from all patients.

Data analysis

The process of texture analyses for the clinical study was identical with those described in the phantom study. To evaluate the differences between texture features of SS and CBM images, % difference (%Diff) was calculated as follows;

$$\%Diff = \left|\frac{TF\_SS - TF\_CBM}{(\mathrm{TF\_SS+TF\_CBM})/2} * 100\right| \ (\%),$$

where TF_SS is the texture feature from SS image and TF_CBM is the texture feature from CBM image. In addition, the Pearson correlation coefficients (r) were calculated to evaluate the agreement of the two scanning techniques. Moreover, for each observer, the %Diff and r values were calculated.

To confirm whether the differences between SS and CBM images were reduced in the clinical settings, we defined the criteria B: (1) %Diff of ≤10%, (2) r value of ≥0.80.

Statistical analysis

Data are expressed as mean ± SD. In the phantom study, the texture features of the SS and the CBM images were compared by a two-tailed paired t-test. An inter-observer difference exists for a feature if a significant difference is found in at least one observer. In the clinical study, a two-tailed unpaired t-test was used to compare the uptake times between the SS and CBM, and a two-tailed paired t-test was used to compare the SUVs and VOI volumes between the two scan techniques. The strength of association was assessed by the Pearson correlation coefficient. An inter-observer difference existed if a texture feature did not fulfill the criteria B in at least one observer. P values of less than 0.05 were considered statistically significant. All analyses were performed using the software JMP ver. 11.2.1.

Result

Phantom study

The significant differences between the texture features of SS and CBM images are shown in Table 2. The detailed values of texture features are provided in Supplementary Table 1–8. Irrespective of resampling method, discrete value, and sphere size, the following 16 features indicated no significant difference between SS and CBM images: energy, contrast, entropy, and dissimilarity for GLCM; low gray-level run emphasis, short-run

low gray-level emphasis, long-run low gray-level emphasis, gray-level non-uniformity (GLNU), and run length non-uniformity for GLRLM; coarseness, contrast, and busyness for NGLDM; short-zone emphasis (SZE), low gray-level zone emphasis, GLNU, and zone percentage (ZP) for GLZLM. Using the FBS discretization, the following four features indicated no significant difference between SS and CBM images irrespective of the discrete value and sphere size: high gray-level run emphasis (HGRE), short-run high gray-level emphasis, long-run high gray-level emphasis (LRHGE) for GLRLM; and zone length non-uniformity (ZLNU) for GLZLM. Using the FBN discretization, the following eight features indicated no significant difference between SS and CBM images irrespective of the discrete value and sphere size: homogeneity for GLCM; short-run emphasis (SRE), long-run emphasis (LRE), and run percentage (RP) for GLRLM; high gray-level zone emphasis, short-zone low gray-level emphasis, short-zone high gray-level emphasis, and long-zone low gray-level emphasis for GLZLM. An inter-observer bias was found between SS and CBM images in ZLNU for GLZLM. The data point has been indicated by an asterisk in Table 2. The p values of two observers were 0.034 and 0.064, respectively.

Regarding the sphere sizes, the number of features with significant differences for the 22, 28, and 37 mm spheres was in the ranges of 1–2, 0–2, and 4–9 depending on resampling conditions (i.e., method and discrete value), respectively. When the sphere size was 37 mm, the number of features with significant differences increased irrespective of the resampling condition.

Regarding the resampling conditions, using the FBS discretization, the number of features with

significant differences increased with the increase in discrete values. When the discrete value was 64 and 128, the number was 5 and 13, respectively. On the contrary, using the FBN discretization, the number was 8 irrespective of the discrete values.

The CV for different settings is shown in Supplementary Figure 1. Firstly, the CV was calculated individually for each observer. Since the CV values between the two observers were very similar and have almost no differences (Supplementary Figure 2), they were therefore merged. Independent of the scan type, resampling condition, and sphere size, the following six features were CV of ≤10%: homogeneity, entropy, dissimilarity for GLCM; SRE, LRE, and RP for GLRLM. Using the FBS discretization, the four features were CV of ≤10% irrespective of the scan type and sphere size: energy and contrast for GLCM; HGRE and LRHGE for GLRLM, although the contrast and LRHGE were limited in the discrete value of 64. Using the FBN discretization, the three features were CV of ≤10% irrespective of the scan type, discrete value, and sphere size: GLNU for GLRLM; SZE and ZP for GLZLM.

Based on these results, the texture features fulfilled the criteria A were listed in Table 3. Among these 13 features, only two entropy and dissimilarity from GLCM fulfilled the criteria A overall resampling conditions. The remaining 11 features depended on the resampling conditions.

Clinical study

The parameters of the two scanning techniques are shown in Table 4. Although there was a significant difference in the uptake times between SS and CBM imaging ($p = 0.018$), the SUVs and VOI volumes did not exhibit significant differences between the two scanning techniques.

Motivated by the results of the phantom study, the texture features met the criteria A were examined in the clinical study. Table 5 shows mean %Diff between the texture features of SS and CBM images in both observers. The following eight features had %Diff of ≤10%: homogeneity, entropy, and dissimilarity for GLCM; SRE, LRE, and RP for GLRLM; SZE and ZP for GLZLM. An inter-observer difference was observed in GLNU from GLRLM because the mean %Diff from observer 2 was over 10%, although no significant differences for discrete values of 64 ($p = 0.15$) and 128 ($p = 0.10$) using a two-tailed paired t-test were found. Table 6 shows correlation coefficients between the texture features of the two scanning techniques in both observers. The following eight features showed r values of ≥0.80: homogeneity, energy, contrast, entropy, and dissimilarity from GLCM; HGRE, LRHGE, GLNU from GLRLM.

Based on these results, the texture features fulfilled the criteria B are listed in Table 7. Both entropy and dissimilarity met the criteria B overall resampling conditions. Homogeneity met the criteria, although the resampling conditions were limited to the FBN discretization.

Discussion

The differences between the texture features of SS and CBM images depended on sphere sizes and resampling conditions in a phantom study. Regarding the sphere sizes, the 22 mm and 28 mm spheres resulted in having between zero and two features with significant differences. In analyzing the 37 mm sphere, a drastically increase in the number of features with significant differences was observed. This might be because of the image noise for each sphere. In our previous study, the variability of SUV increased as the sphere diameter decreased, indicating that the small spheres possess a higher noise than the large ones *(15)*. Pfaehler et al. reported that a larger number of features are sensitive to image noise *(13)*. In the 22 mm and 28 mm spheres, it might be difficult to achieve a statistical significance, since the fluctuations of the feature values were large due to the higher image noise. In the 37 mm sphere, on the other hand, the number of features with significant differences may have increased, since they were small due to the lower image noise, Moreover, the CV of the 37 mm sphere tends to be smaller than those of the other spheres in this phantom study. Therefore, it can be inferred that the subtle differences found between the two techniques were indicated accurately in the 37 mm sphere.

Because the resampling condition has a crucial impact on texture features *(12)*, the two resampling methods and the discrete values were analyzed. When using the FBS discretization, the number of features with significant differences increased when the discrete values increased. Contrarily, the FBN discretization was not influenced by the discrete values. This might be because of the magnitude in the change of bin width. Thus, the change in bin width for FBN discretization was much smaller than that for FBS discretization.

A simple uniform phantom was used in this study in order to investigate the differences of the texture features between SS and CBM techniques. Considering the differences observed in the simple phantom, this clinical study aims to investigate the differences in more detail. We defined the criteria A to find the texture features for the reduction in the differences between SS and CBM images. Thirteen features met the criteria; however, the setting of the phantom study was limited because of the use of uniform objects, a sphere-to-background ratio and radioactivity concentration, and large sphere sizes of 22–37 mm. Therefore, these features were further examined in the clinical settings. For the results, entropy, dissimilarity and homogeneity met the criteria B, indicating high agreement between the two scanning techniques. Among them, both entropy and dissimilarity met the criteria for overall resampling conditions. Especially, the entropy was high because of lower %Diff than that of dissimilarity. The entropy from GLCM has the potential to provide valuable clinical information such as differentiation of malignant and benign bone and soft-tissue lesions, prediction of TN staging, and therapy response in esophageal carcinoma *(6, 8, 18)*. Furthermore, in case of technical aspects, it is independent of reconstruction settings, acquisition modes, and delineation techniques *(8–11)*. In addition, it provides high repeatability and reproducibility *(19, 20)*. This study has successfully demonstrated that entropy from GLCM is robust between SS and CBM techniques. Although this robust feature is grid size and volume dependent, it can still be effectively applied for routine clinical use and in multicenter clinical trials.

Although the %Diff of dissimilarity was slightly worse than that of entropy, the agreement between the two scanning techniques was high irrespective of resampling conditions. The dissimilarity could become the

sub-optimal feature to reduce the differences between the two scanning techniques. In addition, homogeneity from GLCM might be a suitable feature for reducing the differences, although the resampling conditions were limited. All three features were derived from GLCM. The features from GLCM might be insensitive to the subtle differences between SS and CBM images because it is calculated on a small scale of a few voxels as it quantifies relationships between neighbored voxels compared with the other matrices such as GLRLM and GLZLM on a large scale of relatively many voxels.

In the phantom study, the hot spheres were placed with overlapping regions. Although the phantom position could influence the results because the sensitivity of SS technique varies depending on the scanning position *(21)*, the clinical findings concludes that the impact is small as such data were obtained from the various positions.

To study inter-observer differences, texture analyses were performed by two observers. The minor inter-observer differences were observed owing to slight differences in the volume sizes of normal tissues close to the tumor. However, the agreement was strongly correlated, which corresponded with the findings of a similar study *(22)*. Therefore, the LIFEx software can provide textural information without inter-observer bias.

There are limitations of this study. A fixed thresholding method was used in the study. The simple method may lead to be inaccurate tumor delineation because it can underestimate the true tumor volume *(22)*. Additional studies using other delineation tools such as adaptive thresholding or gradient-based method should

be investigated *(23)*, although we suppose that the relative differences between the scanning techniques were not changed. In the clinical study, we did not use respiratory gating even though some lesions were in the lung and upper abdomen which could be affected by respiratory motion. Additionally, although small volumes may not be suitable for texture analysis due to the limited spatial resolution of PET imaging *(24)*, they were still included in the clinical study. Future studies should only include larger lesions.

Conclusion

This study demonstrated that texture analysis was sensitive to scanning techniques. However, the magnitude in differences between texture features of SS and CBM images were different depending on types of features. Because entropy for GLCM exhibits minimal differences between the SS and CBM images irrespective of resampling conditions, it may be a useful feature to be applied for routine clinical use and in multicenter clinical trials.

DISCLOSURE

No potential conflict of interest relevant to this article was reported.

Reference

1. Lim R, Eaton A, Lee NY, et al. ^{18}F-FDG PET/CT metabolic tumor volume and total lesion glycolysis predict outcome in oropharyngeal squamous cell carcinoma. *J Nucl Med*. 2012;53:1506-13.
2. Hatt M, Tixier F, Pierce L, Kinahan PE, Le Rest CC, Visvikis D. Characterization of PET/CT images using texture analysis: the past, the present… any future? *Eur J Nucl Med Mol Imaging*. 2017;44:151-65.
3. Tixier F, Cheze Le Rest, C, Hatt M, et al. Intratumor heterogeneity characterized by textural features on baseline 18F-FDG PET images predicts response to concomitant radio chemotherapy in esophageal cancer. *J Nucl Med*. 2011;52:369-78.
4. Molina-García D, García-Vicente AM, Pérez-Beteta J, et al. Intratumoral heterogeneity in 18F-FDG PET/CT by textural analysis in breast cancer as a predictive and prognostic subrogate. *Ann Nucl Med*. 2018;32:379-88.
5. Cook GJ, O'Brien ME, Siddique M, et al. Non-small cell lung cancer treated with Erlotinib: heterogeneity of 18F-FDG uptake at PET-association with treatment response and prognosis. *Radiology*. 2015;276:883-93.
6. Dong X, Xing L, Wu P, et al. Three-dimensional positron emission tomography image texture analysis of esophageal squamous cell carcinoma: relationship between tumor ^{18}F-fluorodeoxyglucose uptake heterogeneity, maximum standardized uptake value, and tumor stage. *Nucl Med Commun*. 2013;34:40-6.
7. El Naqa I, Grigsby P, Apte A, et al. Exploring feature-based approaches in PET images for predicting cancer treatment outcomes. *Pattern Recognit*.

2009; 42:1162–1171.

8. Hatt M, Tixier F, Cheze Le Rest C, Pradier O, Visvikis D. Robustness of intratumour 18F-FDG PET uptake heterogeneity quantification for therapy response prediction in oesophageal carcinoma. *Eur J Nucl Med Mol Imaging*. 2013;40:1662-71.
9. Galavis PE, Hollensen C, Jallow N, Paliwal B, Jeraj R. Variability of textural features in FDG PET images due to different acquisition modes and reconstruction parameters. *Acta Oncol*. 2010;49:1012-6.
10. Yan J, Lim JC-S, Loi HY, et al. Impact of image reconstruction settings on texture features in 18F-FDG PET. *J Nucl Med*. 2015;56:1667-73.
11. Orlhac F, Soussan M, Maisonobe J-A, Garcia CA, Vanderlinden B, Buvat I. Tumor texture analysis in 18F-FDG PET: relationships between texture parameters, histogram indices, standardized uptake values, metabolic volumes, and total lesion glycolysis. *J Nucl Med*. 2014;55:414-22.
12. Orlhac F, Soussan M, Chouahnia K, Martinod E, Buvat I. 18F-FDG PET-derived textural indices reflect tissue-specific uptake pattern in non-small cell lung cancer. *PLoS ONE*. 2015;10: e0145063.
13. Pfaehler E, Beukinga RJ, de Jong JR, et al. Repeatability of 18F-FDG PET radiomic features: a phantom study to explore sensitivity to image reconstruction settings, noise, and delineation method. *Med Phys*. 2019; 46:665–678
14. Oliver JA, Budzevich M, Zhang GG, Dilling TJ, Latifi K, Moros EG. Variability of image features computed from conventional and respiratory-gated PET/CT images of lung cancer. *Transl Oncol*.

2015;8:524-34.

15. Yamashita S, Yamamoto H, Nakaichi T, Yoneyama T, Yokoyama K. Comparison of image quality between step-and-shoot and continuous bed motion techniques in whole-body (18)F-fluorodeoxyglucose positron emission tomography with the same acquisition duration. *Ann Nucl Med*. 2017;31:686-95.
16. Nioche C, Orlhac F, Boughdad S, et al. LIFEx: a freeware for Radiomic feature calculation in multimodality imaging to accelerate advances in the characterization of tumor heterogeneity. *Cancer Res*. 2018;78:4786-9.
17. Erdi YE, Mawlawi O, Larson SM, et al. Segmentation of lung lesion volume by adaptive positron emission tomography image thresholding. *Cancer*. 1997;80:2505-9.
18. Xu R, Kido S, Suga K, et al. Texture analysis on 18F-FDG PET/CT images to differentiate malignant and benign bone and soft-tissue lesions. *Ann Nucl Med*. 2014;28:926-35.
19. Tixier F, Hatt M, Le Rest CC, Le Pogam A, Corcos L, Visvikis D. Reproducibility of tumor uptake heterogeneity characterization through textural feature analysis in 18F-FDG PET. *J Nucl Med*. 2012;53:693-700.
20. Desseroit MC, Tixier F, Weber W, et al. Reliability of PET/CT shape and heterogeneity features in functional and morphological components of non-small cell lung cancer tumors: a repeatability analysis in a prospective multi-center cohort. *J Nucl Med*. 2017;58:406-11.
21. Rausch I, Cal-Gonzalez J, Dapra D, et al. Performance evaluation of the Biograph mCT flow PET/CT system

according to the NEMA NU2-2012 standard. *EJNMMI Phys*. 2015; 2:26.

22. Guezennec C, Bourhis D, Orlhac F, et al. Inter-observer and segmentation method variability of textural analysis in pre-therapeutic FDG PET/CT in head and neck cancer. Hutson AD, editor. *PLoS One*. 2019;14:e0214299.
23. Hatt M, Lee JA, Schmidtlein CR, et al. Classification and evaluation strategies of auto-segmentation approaches for PET: Report of AAPM task group No.211. *Med Phys*. 2017;44:e1-e42.
24. Hatt M, Majdoub M, Vallières M, et al. 18F-FDG PET uptake characterization through texture analysis: investigating the complementary nature of heterogeneity and functional tumor volume in a multi-cancer site patient cohort. *J Nucl Med*. 2015;56:38-44.

TABLE 1. Texture features

Matrix	Feature
Gray-Level Co-occurrence Matrix (GLCM)	Homogeneity
	Energy
	Contrast
	Correlation
	Entropy_log10
	Dissimilarity
Gray-Level Run Length Matrix (GLRLM)	Short-Run Emphasis(SRE)
	Long-Run Emphasis (LRE)
	Low Gray-level Run Emphasis (LGRE)
	High Gray-level Run Emphasis (HGRE)
	Short-Run Low Gray-level Emphasis (SRLGE)
	Short-Run High Gray-level Emphasis (SRHGE)
	Long-Run Low Gray-level Emphasis (LRLGE)
	Long-Run High Gray-level Emphasis (LRHGE)
	Gray-Level Non-Uniformity (GLNU)
	Run Length Non-Uniformity (RLNU)
	Run Percentage (RP)
Neighborhood Gray-Level Different Matirx (NGLDM)	Coarseness
	Contrast
	Busyness
Gray-Level Zone Length Matrix (GLZLM)	Short-Zone Emphasis(SZE)
	Long-Zone Emphasis (LZE)
	Low Gray-level Zone Emphasis (LGZE)
	High Gray-level Zone Emphasis (HGZE)
	Short-Zone Low Gray-level Emphasis (SZLGE)
	Short-Zone High Gray-level Emphasis (SZHGE)
	Long-Zone Low Gray-level Emphasis (LZLGE)
	Long-Zone High Gray-level Emphasis (LZHGE)
	Gray-Level Non-Uniformity (GLNU)
	Zone Length Non-Uniformity (ZLNU)
	Zone Percentage (ZP)

TABLE 2. Significant differences between the texture features of SS and CBM images.

Resampling method	Discrete value	Sphere size [mm]	GLCM						GLRLM											NGLDM			GLZLM										
			Homogeneity	Energy	Contrast	Correlation	Entropy_log10	Dissimilarity	SRE	LRE	LGRE	HGRE	SRLGE	SRHGE	LRLGE	LRHGE	GLNU	RLNU	RP	Coarseness	Contrast	Busyness	SZE	LZE	LGZE	HGZE	SZLGE	SZHGE	LZLGE	LZHGE	GLNU	ZLNU	ZP
FBS	64	2	-	-	-	+	-	-	-	-	-	-	-	-	-	-	-	-	-	-	-	-	-	-	-	-	-	-	-	-	-	-	-
		2	-	-	-	-	-	-	-	-	-	-	-	-	-	-	-	-	-	-	-	-	-	-	-	-	-	-	-	-	-	-	-
		2																															
		8																															
		3	+	-	-	-	-	-	+	+	-	-	-	-	-	-	-	-	+	-	-	-	-	-	-	-	-	-	-	-	-	-	-
		7																															
	128	2	-	-	-	+	-	-	-	-	-	-	-	-	-	-	-	-	-	-	-	-	-	-	-	-	-	+	-	-	-	-	-
		2																															
		2	-	-	-	-	-	-	-	+	-	-	-	-	-	-	-	-	+	-	-	-	-	-	-	-	-	-	-	-	-	-	-
		8																															
		3	+	-	-	-	-	-	+	+	-	-	-	-	-	-	-	-	+	-	-	-	-	+	-	+	+	-	+	+	-	-	-
		7																															
FBN	64	2	-	-	-	+	-	-	-	-	-	-	-	-	-	-	-	-	-	-	-	-	-	-	-	-	-	-	-	-	-	-	-
		2	-	-	-	-	-	-	-	-	-	-	-	-	-	-	-	-	-	-	-	-	-	-	-	-	-	-	-	-	-	-	-
		2																															
		8																															
		3	-	-	-	+	-	-	-	-	-	+	-	+	-	+	-	-	-	-	-	-	-	+	-	-	-	-	-	+	-	+	-
		7																															

128	22	-	-	-	+	-	-		-	-	-	-	-	-	-	-	-	-	-		-	-	-		-	-	-	-	-	-	-	-	-	-	-
	28	-	-	-	-	-	-		-	-	-	-	-	-	-	-	-	-	-		-	-	-		-	-	-	-	-	-	-	+	-	-	-
	37	-	-	-	+	-	-		-	-	-	+	-	+	-	+	-	-	-		-	-	-		-	-	-	-	-	-	-	+	-	+*	-

Abbreviations of the texture features are listed in Table 1. FBS, fixed bin size; FBN, fixed bin number. + = significant difference; - = nonsignificant difference. *：confirmed inter-observer difference.

TABLE 3. Texture features fulfilling criteria A for both observers.

		GLCM					GLRLM						GLZLM	
Resampling method	Discrete value	Homogeneity	Energy	Contrast	Entropy	Dissimilarity	SRE	LRE	HGRE	LRHGE	GLNU	RP	SZE	ZP
FBS	64	-	○	○	○	○	-	-	○	○	-	-	-	-
	128	-	○	-	○	○	-	-	○	-	-	-	-	-
FBN	64	○	-	-	○	○	○	○	-	-	○	○	○	○
	128	○	-	-	○	○	○	○	-	-	○	○	○	○

Abbreviations of the texture features are listed in Table 1. FBS, fixed bin size; FBN, fixed bin number.

TABLE 4. Parameters of SS and CBM techniques

	SS	CBM	p value
Uptake time (min)	68.7 ± 6.5	63.1 ± 7.8	0.018
SUVmean	5.4 ± 3.8	5.4 ± 3.8	0.933
SUVmax	8.5 ± 5.6	8.6 ± 5.7	0.628
VOI volume (mL)	16.0 ± 22.8	15.9 ± 22.7	0.915

Abbreviations: SS, step-and-shoot; CBM, continuous bed motion; SUV, standardized uptake value; VOI, volume of interest

TABLE 5. %Diff between texture features of SS and CBM images derived from two observers

Observer	Resampling method	Discrete value	GLCM					GLRLM						GLZLM	
			Homogeneity	Energy	Contrast	Entropy	Dissimilarity	SRE	LRE	HGRE	LRHGE	GLNU	RP	SZE	ZP
1	FBS	64	-	17.36 ± 27.71	16.40 ± 14.37	3.18 ± 3.18	8.78 ± 7.32	-	-	12.84 ± 8.19	12.31 ± 9.66	-	-	-	-
		128	-	15.56 ± 29.52	-	2.49 ± 2.69	8.97 ± 7.33	-	-	12.99 ± 8.06	-	-	-	-	-
	FBN	64	7.10 ± 4.78	-	-	2.51 ± 2.03	7.08 ± 5.02	0.28 ± 0.18	1.07 ± 0.75	-	-	*8.55 ± 7.52	0.36 ± 0.24	3.29 ± 1.98	4.61 ± 2.88
		128	8.92 ± 6.17	-	-	2.52 ± 2.03	7.01 ± 5.02	0.22 ± 0.15	0.89 ± 0.61	-	-	*8.53 ± 6.74	0.30 ± 0.20	2.77 ± 1.88	3.85 ± 2.62
2	FBS	64	-	17.73 ± 27.70	16.80 ± 13.63	3.16 ± 3.21	8.80 ± 7.21	-	-	12.74 ± 8.91	12.47 ± 9.89	-	-	-	-
		128	-	16.11 ± 29.58	-	2.54 ± 2.73	8.85 ± 7.32	-	-	12.87 ± 8.81	-	-	-	-	-
	FBN	64	7.51 ± 5.72	-	-	2.88 ± 2.50	7.44 ± 5.19	0.27 ± 0.21	1.11 ± 0.80	-	-	*11.41 ± 10.76	0.37 ± 0.27	3.30 ± 2.63	4.65 ± 3.46
		128	9.44 ± 6.81	-	-	2.89 ± 2.58	7.37 ± 5.20	0.22 ± 0.16	0.89 ± 0.63	-	-	*11.02 ± 8.83	0.30 ± 0.21	2.82 ± 2.05	3.82 ± 2.62

Abbreviations of the texture features are listed in Table 1. FBS, fixed bin size; FBN, fixed bin number. *: confirmed inter-observer difference

TABLE 6. Correlation between texture features of SS and CBM images derived from two observers

Observer	Resampling method	Discrete value	GLCM					GLRLM						GLZLM	
			Homogeneity	Energy	Contrast	Entropy	Dissimilarity	SRE	LRE	HGRE	LRHGE	GLNU	RP	SZE	ZP
1	FBS	64	-	0.96 (<0.001)	0.99 (<0.001)	0.97 (<0.001)	0.99 (<0.001)	-	-	0.99 (<0.001)	0.95 (<0.001)	-	-	-	-
		128	-	0.87 (<0.001)	-	0.96 (<0.001)	0.99 (<0.001)	-	-	0.99 (<0.001)	-	-	-	-	-
	FBN	64	0.88 (<0.001)	-	-	0.98 (<0.001)	0.90 (<0.001)	0.66 (<0.001)	0.63 (<0.001)	-	-	1.00 (<0.001)	0.66 (<0.001)	0.61 (<0.001)	0.70 (<0.001)
		128	0.83 (<0.001)	-	-	0.98 (<0.001)	0.90 (<0.001)	0.27 (0.170)	0.17 (0.391)	-	-	1.00 (<0.001)	0.31 (0.115)	0.23 (0.258)	0.29 (0.141)
2	FBS	64	-	0.96 (<0.001)	0.99 (<0.001)	0.97 (<0.001)	0.99 (<0.001)	-	-	0.99 (<0.001)	0.95 (<0.001)	-	-	-	-
		128	-	0.87 (<0.001)	-	0.96 (<0.001)	0.99 (<0.001)	-	-	0.99 (<0.001)	-	-	-	-	-
	FBN	64	0.84 (<0.001)	-	-	0.97 (<0.001)	0.88 (<0.001)	0.62 (<0.001)	0.62 (<0.001)	-	-	1.00 (<0.001)	0.64 (<0.001)	0.53 (0.005)	0.65 (<0.001)
		128	0.80 (<0.001)	-	-	0.97 (<0.001)	0.88 (<0.001)	0.23 (0.244)	0.08 (0.696)	-	-	1.00 (<0.001)	0.25 (0.200)	0.19 (0.340)	0.28 (0.161)

Abbreviations of the texture features are listed in Table 1. FBS, fixed bin size; FBN, fixed bin number. Data expressed as r value (p value)

TABLE 7. Texture features fulfilling criteria B for both observers.

		GLCM		
Resampling method	Discrete value	Homogeneity	Entropy	Dissimilarity
FBS	64	-	○	○
	128	-	○	○
FBN	64	○	○	○
	128	○	○	○

Abbreviation: GLCM, gray-level co-occurrence matrix; FBS, fixed bin size; FBN, fixed bin number.

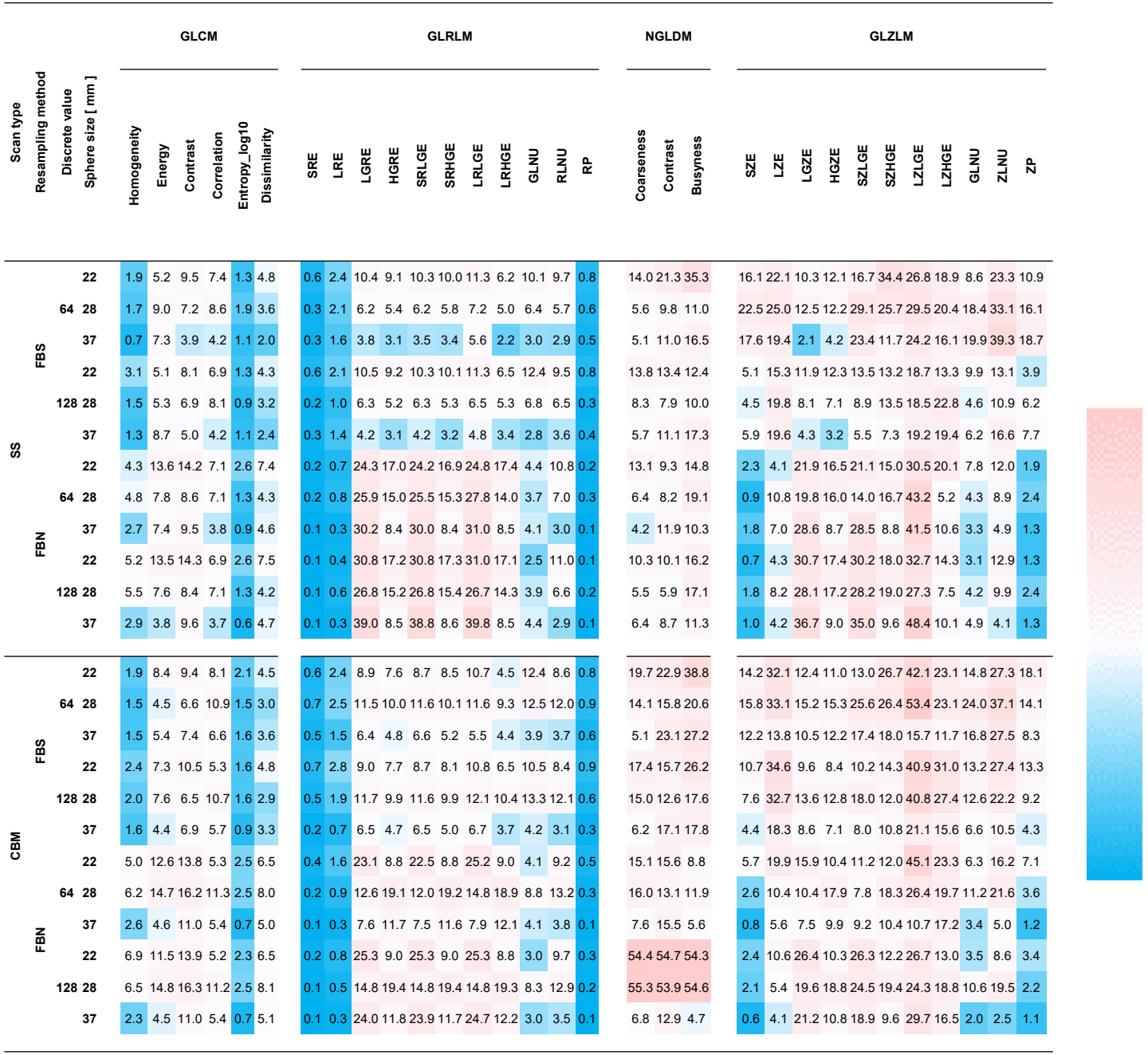

Supplementary Figure 1. Heat map showing the coefficient of variation for different settings. Abbreviations of the texture features are listed in Table 1. SS, step-and-shoot, CBM, continuous bed motion, FBS, fixed bin size, FBN, fixed bin number.

Scan type	Resampling method	Discrete value	Sphere size [mm]	GLCM						GLRLM										NGLDM			GLZLM										
				Homogeneity	Energy	Contrast	Correlation	Entropy_log10	Dissimilarity	SRE	LRE	LGRE	HGRE	SRLGE	SRHGE	LRLGE	LRHGE	GLNU	RLNU	RP	Coarseness	Contrast	Busyness	SZE	LZE	LGZE	HGZE	SZLGE	SZHGE	LZLGE	LZHGE	GLNU	ZLNU	ZP
SS	FBS	64	22	0.0	0.0	0.0	0.0	0.0	0.0	0.0	0.0	0.0	0.0	0.0	0.0	0.0	0.0	0.0	0.0	0.0	0.0	0.0	0.0	0.0	0.0	0.0	0.0	0.0	0.0	0.0	0.0	0.0	0.0	0.0
			28	0.0	0.0	0.0	0.0	0.0	0.0	0.0	0.0	0.0	0.0	0.0	0.0	0.0	0.0	0.0	0.0	0.0	0.0	0.0	0.0	0.0	0.0	0.0	0.0	0.0	0.0	0.0	0.0	0.0	0.0	0.0
			37	0.0	0.0	0.0	0.0	0.0	0.0	0.0	0.0	0.0	0.0	0.0	0.0	0.0	0.0	0.0	0.0	0.0	0.0	0.0	0.0	0.0	0.0	0.0	0.0	0.0	0.0	0.0	0.0	0.0	0.0	0.0
		128	22	0.0	0.0	0.0	0.0	0.0	0.0	0.0	0.0	0.0	0.0	0.0	0.0	0.0	0.0	0.0	0.0	0.0	0.0	0.0	0.0	0.0	0.0	0.0	0.0	0.0	0.0	0.0	0.0	0.0	0.0	0.0
			28	0.0	0.0	0.0	0.0	0.0	0.0	0.0	0.0	0.0	0.0	0.0	0.0	0.0	0.0	0.0	0.0	0.0	0.0	0.0	0.0	0.0	0.0	0.0	0.0	0.0	0.0	0.0	0.0	0.0	0.0	0.0
			37	0.0	0.0	0.0	0.0	0.0	0.0	0.0	0.0	0.0	0.0	0.0	0.0	0.0	0.0	0.0	0.0	0.0	0.0	0.0	0.0	0.0	0.0	−0.1	0.2	0.0	0.0	0.0	0.0	0.1	0.0	−0.2
	FBN	64	22	0.0	0.0	0.0	0.0	0.0	0.0	0.0	0.0	0.0	0.0	0.0	0.0	0.0	0.0	0.0	0.0	0.0	0.0	0.0	0.0	0.1	0.2	0.0	0.0	0.0	0.0	0.0	0.0	0.1	0.0	0.0
			28	0.0	0.0	0.0	0.0	0.0	0.0	0.0	0.0	0.0	0.0	0.0	0.0	0.0	0.0	0.0	0.0	0.0	0.0	0.0	0.0	0.0	0.0	0.0	0.0	0.0	0.0	0.0	0.0	0.0	0.0	0.0
			37	0.0	0.0	0.0	0.0	0.0	0.0	0.0	0.0	0.0	0.0	0.0	0.0	0.0	0.0	0.0	0.0	0.0	0.0	0.0	0.0	0.0	0.0	0.0	0.1	0.0	0.1	0.0	0.1	0.0	0.1	0.0
		128	22	0.0	0.0	0.0	0.0	0.0	0.0	0.0	0.0	0.0	0.0	0.0	0.0	0.0	0.0	0.0	0.0	0.0	0.0	0.0	0.0	0.0	0.0	0.0	0.0	0.0	0.0	0.0	0.0	0.0	0.0	0.0
			28	0.0	0.0	0.0	0.0	0.0	0.0	0.0	0.0	0.0	0.0	0.0	0.0	0.0	0.0	0.0	0.0	0.0	0.0	0.0	0.0	0.0	0.0	0.0	0.0	0.0	0.0	0.0	0.0	0.0	0.0	0.0
			37	0.0	0.0	0.0	0.0	0.0	0.0	0.0	0.0	0.0	0.0	0.0	0.0	0.0	0.0	0.0	0.0	0.0	0.0	0.0	0.0	0.0	−0.1	0.1	0.0	−0.1	0.0	−0.1	0.0	0.0	−1.0	−0.4	0.0
CBM	FBS	64	22	0.0	0.0	0.0	0.0	0.0	0.0	0.0	0.0	0.0	0.0	0.0	0.0	0.0	0.0	0.0	0.0	0.0	0.0	0.0	0.0	0.0	0.0	0.0	0.0	0.0	0.0	0.0	0.0	0.0	0.0	0.0
			28	0.1	0.0	0.0	0.0	0.0	0.0	0.0	0.0	0.0	0.0	0.0	0.0	0.1	−0.1	0.0	0.0	0.0	0.1	0.0	0.3	0.0	0.2	0.0	0.0	0.0	0.0	0.4	0.1	0.0	0.0	0.1
			37	0.0	0.0	0.0	0.0	0.0	0.0	0.0	0.0	0.0	0.0	0.0	0.0	0.0	0.0	0.0	0.0	0.0	0.0	0.0	0.0	0.0	0.0	0.0	0.0	0.0	0.0	0.0	0.0	0.0	0.0	0.0
		128	22	0.0	0.0	0.0	0.0	0.0	0.0	0.0	0.0	0.0	0.0	0.0	0.0	0.0	0.0	0.0	0.0	0.0	0.0	0.0	0.0	0.0	0.0	0.0	0.0	0.0	0.0	0.0	0.0	0.0	0.0	0.0
			28	0.1	0.0	0.0	0.0	0.0	0.0	0.0	0.0	0.0	0.0	0.0	0.0	0.1	0.0	0.1	0.0	0.0	0.0	0.0	0.2	−0.1	0.6	0.0	0.3	0.1	−0.5	0.0	−0.1	0.6	0.1	0.0	0.0	0.3
			37	0.0	0.0	0.0	0.0	0.0	0.0	0.0	0.0	0.0	0.0	0.0	0.0	0.0	0.0	0.0	0.0	0.0	0.0	0.0	0.0	0.0	0.0	0.0	0.0	0.0	0.0	0.0	0.0	0.0	0.0	0.0	0.0	0.0
	FBN	64	22	0.0	−0.1	0.1	0.0	0.0	0.0	0.0	0.1	2.5	0.0	2.5	0.0	2.6	−0.1	2.1	−0.1	0.0	1.9	0.1	1.9	0.0	0.0	3.6	0.3	−1.4	0.3	2.9	−0.9	−1.1	0.0	0.0
			28	0.1	0.0	0.0	−0.1	0.0	0.0	0.0	0.0	0.5	0.0	0.5	0.0	0.5	0.0	0.1	0.0	0.0	0.0	0.0	0.3	0.0	0.2	0.7	0.0	0.9	0.1	0.5	−0.1	0.0	0.0	0.0
			37	0.0	0.0	0.0	0.0	0.0	0.0	0.0	0.0	0.0	0.0	0.0	0.0	0.0	0.0	0.0	0.0	0.0	0.0	0.0	0.0	−0.2	0.1	0.0	0.2	0.0	0.3	0.0	0.0	0.0	−0.1	0.1
		128	22	0.2	−0.2	0.1	0.0	0.0	0.1	0.0	0.2	1.1	−0.1	1.1	−0.1	1.1	0.0	1.3	−0.2	0.1	0.8	0.0	0.3	0.8	2.5	2.1	0.2	2.0	0.0	2.2	1.8	−0.4	−0.1	0.9
			28	0.1	0.0	0.0	−0.1	0.0	0.0	0.0	0.0	0.1	0.0	0.1	0.0	0.0	0.0	0.0	0.0	0.0	0.0	0.0	0.1	0.0	0.0	0.2	0.0	0.3	0.0	0.1	0.0	0.0	0.1	0.0
			37	0.0	0.0	0.0	0.0	0.0	0.0	0.0	0.0	0.0	0.0	0.0	0.0	0.0	0.0	0.0	0.0	0.0	0.0	0.0	0.0	0.0	0.0	0.0	0.1	0.0	0.1	0.0	0.1	0.0	0.1	0.0

Supplementary Figure 2. Subtraction of CV values for observer 2 from observer 1. Abbreviations of the texture features are listed in Table 1. SS, step-and-shoot, CBM, continuous bed motion, FBS, fixed bin size, FBN, fixed bin number.

Supplementary Table 1. Texture feature values of step-and-shoot images using fixed bin size discretization derived from observer 1.

	discrete value 64			discrete value 128		
	22 mm	28mm	37mm	22 mm	28mm	37mm
GLCM_Homogeneity	4.41E-01±8.94E-03	4.68E-01±8.26E-03	5.03E-01±3.81E-03	3.04E-01±1.01E-02	3.30E-01±5.20E-03	3.58E-01±4.81E-03
GLCM_Energy	2.53E-02±1.39E-03	2.40E-02±2.30E-03	2.76E-02±2.12E-03	1.17E-02±6.28E-04	8.67E-03±4.84E-04	8.17E-03±7.55E-04
GLCM_Contrast	6.67E+00±6.70E-01	5.78E+00±4.42E-01	4.54E+00±1.89E-01	2.61E+01±2.25E+00	2.26E+01±1.66E+00	1.78E+01±9.39E-01
GLCM_Correlation	2.63E-01±2.07E-02	3.52E-01±3.19E-02	4.18E-01±1.85E-02	2.66E-01±1.94E-02	3.54E-01±3.05E-02	4.21E-01±1.86E-02
GLCM_Entropy_log10	1.66E+00±2.24E-02	1.71E+00±3.36E-02	1.68E+00±1.97E-02	1.99E+00±2.83E-02	2.15E+00±2.09E-02	2.20E+00±2.52E-02
GLCM_Dissimilarity	2.06E+00±1.04E-01	1.88E+00±7.25E-02	1.63E+00±3.39E-02	4.12E+00±1.90E-01	3.75E+00±1.28E-01	3.27E+00±8.31E-02
GLRLM_SRE	9.19E-01±6.11E-03	9.01E-01±3.15E-03	8.77E-01±3.16E-03	9.60E-01±6.25E-03	9.48E-01±2.35E-03	9.36E-01±2.88E-03
GLRLM_LRE	1.37E+00±3.56E-02	1.51E+00±3.33E-02	1.70E+00±2.91E-02	1.17E+00±2.65E-02	1.23E+00±1.28E-02	1.31E+00±1.95E-02
GLRLM_LGRE	1.36E-02±1.51E-03	1.21E-02±7.97E-04	1.06E-02±4.28E-04	3.58E-03±4.01E-04	3.15E-03±2.10E-04	2.75E-03±1.24E-04
GLRLM_HGRE	9.01E+01±8.66E+00	1.01E+02±5.80E+00	1.13E+02±3.75E+00	3.45E+02±3.37E+01	3.91E+02±2.18E+01	4.38E+02±1.46E+01
GLRLM_SRLGE	1.27E-02±1.39E-03	1.12E-02±7.29E-04	9.54E-03±3.54E-04	3.46E-03±3.80E-04	3.02E-03±2.02E-04	2.61E-03±1.17E-04
GLRLM_SRHGE	8.18E+01±8.68E+00	8.93E+01±5.50E+00	9.68E+01±3.48E+00	3.28E+02±3.52E+01	3.67E+02±2.05E+01	4.06E+02±1.36E+01
GLRLM_LRLGE	1.80E-02±2.16E-03	1.70E-02±1.30E-03	1.65E-02±9.74E-04	4.12E-03±4.93E-04	3.74E-03±2.58E-04	3.43E-03±1.75E-04
GLRLM_LRHGE	1.29E+02±8.45E+00	1.64E+02±8.63E+00	2.08E+02±4.80E+00	4.16E+02±2.85E+01	5.01E+02±2.79E+01	5.94E+02±2.13E+01
GLRLM_GLNU	1.68E+01±1.79E+00	2.84E+01±1.94E+00	6.32E+01±2.02E+00	9.58E+00±1.26E+00	1.61E+01±1.16E+00	3.61E+01±1.06E+00
GLRLM_RLNU	9.26E+01±9.53E+00	1.68E+02±1.02E+01	3.50E+02±1.10E+01	1.08E+02±1.09E+01	2.04E+02±1.41E+01	4.45E+02±1.72E+01
GLRLM_RP	8.98E-01±7.66E-03	8.70E-01±5.85E-03	8.35E-01±4.10E-03	9.48E-01±7.57E-03	9.32E-01±3.01E-03	9.14E-01±4.33E-03
NGLDM_Coarseness	3.77E-02±5.60E-03	2.39E-02±1.43E-03	1.23E-02±6.63E-04	3.46E-02±5.09E-03	2.22E-02±1.95E-03	1.18E-02±7.15E-04
NGLDM_Contrast	1.82E-01±4.12E-02	1.62E-01±1.69E-02	1.33E-01±1.56E-02	3.86E-01±5.47E-02	3.54E-01±2.94E-02	2.67E-01±3.14E-02
NGLDM_Busyness	1.38E+00±5.18E-01	1.40E+00±1.64E-01	2.23E+00±3.91E-01	4.20E-01±5.52E-02	4.67E-01±4.97E-02	6.43E-01±1.18E-01
GLZLM_SZE	4.69E-01±8.03E-02	4.32E-01±1.03E-01	3.90E-01±7.30E-02	6.46E-01±3.52E-02	5.92E-01±2.86E-02	6.00E-01±3.77E-02
GLZLM_LZE	5.11E+01±1.20E+01	1.17E+02±3.10E+01	4.94E+02±1.02E+02	7.23E+00±1.18E+00	1.62E+01±3.40E+00	5.59E+01±1.16E+01
GLZLM_LGZE	1.55E-02±1.69E-03	1.54E-02±2.04E-03	1.37E-02±3.07E-04	3.81E-03±4.82E-04	3.60E-03±3.09E-04	3.34E-03±1.52E-04
GLZLM_HGZE	8.22E+01±1.06E+01	8.31E+01±1.07E+01	9.00E+01±4.03E+00	3.21E+02±4.17E+01	3.41E+02±2.57E+01	3.63E+02±1.27E+01
GLZLM_SZLGE	8.16E-03±1.45E-03	7.72E-03±2.38E-03	5.53E-03±1.37E-03	2.54E-03±3.63E-04	2.26E-03±2.12E-04	2.08E-03±1.21E-04
GLZLM_SZHGE	3.48E+01±1.27E+01	3.16E+01±8.59E+00	3.47E+01±4.32E+00	1.99E+02±2.78E+01	1.91E+02±2.74E+01	2.09E+02±1.63E+01
GLZLM_LZLGE	6.82E-01±1.94E-01	1.12E+00±3.50E-01	3.91E+00±1.00E+00	2.37E-02±4.69E-03	3.78E-02±7.43E-03	1.09E-01±2.22E-02
GLZLM_LZHGE	4.62E+03±9.27E+02	1.40E+04±3.03E+03	6.72E+04±1.15E+04	2.74E+03±3.86E+02	8.00E+03±1.93E+03	3.06E+04±6.27E+03
GLZLM_GLNU	4.38E+00±3.99E-01	7.34E+00±1.43E+00	1.20E+01±2.54E+00	5.31E+00±5.58E-01	8.07E+00±3.95E-01	1.40E+01±9.33E-01
GLZLM_ZLNU	6.44E+00±1.59E+00	9.03E+00±3.17E+00	1.11E+01±4.62E+00	2.49E+01±3.46E+00	3.43E+01±3.97E+00	6.13E+01±1.08E+01
GLZLM_ZP	2.16E-01±2.49E-02	1.69E-01±2.89E-02	1.11E-01±2.19E-02	4.97E-01±2.04E-02	4.06E-01±2.68E-02	3.10E-01±2.52E-02

Supplementary Table 2. Texture feature values of step-and-shoot images using fixed bin number discretization derived from observer 1.

	discrete value 64			discrete value 128		
	22 mm	28mm	37mm	22 mm	28mm	37mm
GLCM_Homogeneity	1.25E-01±5.72E-03	1.43E-01±7.28E-03	1.62E-01±4.59E-03	7.64E-02±4.25E-03	8.69E-02±5.04E-03	1.00E-01±3.08E-03
GLCM_Energy	6.71E-03±9.67E-04	3.31E-03±2.72E-04	1.69E-03±1.33E-04	6.41E-03±9.20E-04	2.96E-03±2.39E-04	1.27E-03±5.16E-05
GLCM_Contrast	4.17E+02±6.28E+01	3.37E+02±3.06E+01	2.46E+02±2.49E+01	1.67E+03±2.53E+02	1.35E+03±1.20E+02	9.84E+02±9.99E+01
GLCM_Correlation	2.67E-01±2.00E-02	3.56E-01±2.69E-02	4.24E-01±1.69E-02	2.67E-01±1.96E-02	3.56E-01±2.68E-02	4.24E-01±1.68E-02
GLCM_Entropy_log10	2.19E+00±6.09E-02	2.50E+00±3.40E-02	2.82E+00±2.74E-02	2.20E+00±6.04E-02	2.54E+00±3.45E-02	2.91E+00±1.71E-02
GLCM_Dissimilarity	1.65E+01±1.30E+00	1.45E+01±6.58E-01	1.22E+01±5.99E-01	3.30E+01±2.61E+00	2.90E+01±1.29E+00	2.44E+01±1.21E+00
GLRLM_SRE	9.89E-01±2.03E-03	9.86E-01±2.11E-03	9.82E-01±8.24E-04	9.94E-01±9.81E-04	9.94E-01±1.33E-03	9.91E-01±8.09E-04
GLRLM_LRE	1.04E+00±7.29E-03	1.06E+00±9.14E-03	1.08E+00±3.26E-03	1.02E+00±3.92E-03	1.03E+00±6.26E-03	1.04E+00±3.01E-03
GLRLM_LGRE	5.00E-02±1.29E-02	4.65E-02±1.28E-02	3.04E-02±9.74E-03	2.79E-02±9.13E-03	2.68E-02±7.60E-03	1.53E-02±6.33E-03
GLRLM_HGRE	8.65E+02±1.56E+02	1.03E+03±1.63E+02	1.11E+03±9.92E+01	3.42E+03±6.26E+02	4.06E+03±6.53E+02	4.38E+03±3.97E+02
GLRLM_SRLGE	4.98E-02±1.28E-02	4.61E-02±1.24E-02	3.02E-02±9.60E-03	2.79E-02±9.11E-03	2.67E-02±7.60E-03	1.52E-02±6.27E-03
GLRLM_SRHGE	8.51E+02±1.53E+02	1.01E+03±1.63E+02	1.08E+03±9.66E+01	3.39E+03±6.21E+02	4.03E+03±6.57E+02	4.33E+03±3.93E+02
GLRLM_LRLGE	5.08E-02±1.34E-02	4.83E-02±1.42E-02	3.15E-02±1.03E-02	2.80E-02±9.21E-03	2.68E-02±7.60E-03	1.55E-02±6.55E-03
GLRLM_LRHGE	9.24E+02±1.71E+02	1.11E+03±1.64E+02	1.22E+03±1.09E+02	3.55E+03±6.43E+02	4.20E+03±6.38E+02	4.60E+03±4.14E+02
GLRLM_GLNU	3.15E+00±1.48E-01	5.20E+00±2.06E-01	1.14E+01±4.97E-01	2.05E+00±5.35E-02	3.06E+00±1.27E-01	6.23E+00±2.88E-01
GLRLM_RLNU	1.21E+02±1.39E+01	2.37E+02±1.76E+01	5.35E+02±1.71E+01	1.24E+02±1.44E+01	2.44E+02±1.71E+01	5.55E+02±1.73E+01
GLRLM_RP	9.86E-01±2.46E-03	9.81E-01±2.84E-03	9.76E-01±9.98E-04	9.93E-01±1.27E-03	9.92E-01±1.91E-03	9.88E-01±1.00E-03
NGLDM_Coarseness	2.70E-02±3.76E-03	1.83E-02±1.24E-03	1.07E-02±4.70E-04	2.09E-02±2.28E-03	1.59E-02±9.27E-04	9.90E-03±6.77E-04
NGLDM_Contrast	1.88E+00±1.85E-01	1.59E+00±1.38E-01	1.13E+00±1.42E-01	3.81E+00±4.07E-01	3.33E+00±2.08E-01	2.43E+00±2.25E-01
NGLDM_Busyness	4.53E-02±7.13E-03	4.30E-02±8.70E-03	6.00E-02±6.58E-03	2.43E-02±4.17E-03	1.44E-02±2.60E-03	1.69E-02±2.02E-03
GLZLM_SZE	8.79E-01±2.18E-02	8.55E-01±7.98E-03	8.20E-01±1.60E-02	9.39E-01±7.29E-03	9.28E-01±1.73E-02	8.96E-01±8.73E-03
GLZLM_LZE	1.71E+00±7.50E-02	2.10E+00±2.40E-01	2.83E+00±2.09E-01	1.33E+00±6.06E-02	1.39E+00±1.21E-01	1.65E+00±7.45E-02
GLZLM_LGZE	5.51E-02±1.28E-02	4.97E-02±1.04E-02	3.58E-02±1.09E-02	3.00E-02±9.76E-03	2.94E-02±8.75E-03	1.68E-02±6.55E-03
GLZLM_HGZE	8.01E+02±1.40E+02	9.46E+02±1.60E+02	1.00E+03±9.26E+01	3.27E+03±6.05E+02	3.92E+03±7.15E+02	4.15E+03±3.95E+02
GLZLM_SZLGE	5.22E-02±1.16E-02	4.33E-02±6.43E-03	3.26E-02±9.85E-03	2.96E-02±9.48E-03	2.93E-02±8.75E-03	1.61E-02±5.97E-03
GLZLM_SZHGE	6.58E+02±1.05E+02	7.71E+02±1.37E+02	7.73E+02±7.22E+01	2.98E+03±5.70E+02	3.53E+03±7.11E+02	3.56E+03±3.61E+02
GLZLM_LZLGE	6.90E-02±2.23E-02	7.99E-02±3.66E-02	5.70E-02±2.51E-02	3.15E-02±1.09E-02	3.01E-02±8.72E-03	2.04E-02±1.04E-02
GLZLM_LZHGE	1.72E+03±3.66E+02	2.51E+03±1.37E+02	3.79E+03±4.26E+02	5.06E+03±7.69E+02	6.09E+03±4.82E+02	8.00E+03±8.59E+02
GLZLM_GLNU	2.66E+00±2.21E-01	4.14E+00±1.90E-01	8.14E+00±2.82E-01	1.83E+00±6.05E-02	2.75E+00±1.24E-01	5.21E+00±2.46E-01
GLZLM_ZLNU	7.72E+01±9.85E+00	1.36E+02±1.27E+01	2.62E+02±1.36E+01	9.88E+01±1.35E+01	1.87E+02±1.96E+01	3.73E+02±1.56E+01
GLZLM_ZP	8.34E-01±1.71E-02	7.88E-01±2.00E-02	7.25E-01±9.73E-03	9.12E-01±1.23E-02	8.99E-01±2.27E-02	8.51E-01±1.19E-02

Supplementary Table 3. Texture feature values of continuous bed motion images using fixed bin size discretization derived from observer 1.

	discrete value 64			discrete value 128		
	22 mm	28mm	37mm	22 mm	28mm	37mm
GLCM_Homogeneity	4.33E-01±8.83E-03	4.64E-01±7.41E-03	4.91E-01±7.65E-03	2.96E-01±7.58E-03	3.24E-01±6.97E-03	3.48E-01±5.79E-03
GLCM_Energy	2.55E-02±2.27E-03	2.37E-02±1.13E-03	2.59E-02±1.48E-03	1.18E-02±9.16E-04	8.61E-03±6.96E-04	7.74E-03±3.61E-04
GLCM_Contrast	7.21E+00±7.17E-01	5.85E+00±4.09E-01	4.80E+00±3.77E-01	2.86E+01±3.18E+00	2.28E+01±1.58E+00	1.87E+01±1.37E+00
GLCM_Correlation	2.29E-01±1.96E-02	3.25E-01±3.75E-02	3.75E-01±2.61E-02	2.33E-01±1.31E-02	3.28E-01±3.71E-02	3.84E-01±2.32E-02
GLCM_Entropy_log10	1.67E+00±3.68E-02	1.71E+00±2.68E-02	1.70E+00±2.95E-02	1.98E+00±3.30E-02	2.14E+00±3.64E-02	2.22E+00±2.06E-02
GLCM_Dissimilarity	2.13E+00±1.01E-01	1.89E+00±6.08E-02	1.69E+00±6.44E-02	4.29E+00±2.18E-01	3.78E+00±1.16E-01	3.38E+00±1.17E-01
GLRLM_SRE	9.24E-01±5.89E-03	9.04E-01±6.67E-03	8.85E-01±4.37E-03	9.64E-01±7.28E-03	9.52E-01±4.96E-03	9.41E-01±1.96E-03
GLRLM_LRE	1.35E+00±3.41E-02	1.48E+00±3.96E-02	1.63E+00±2.51E-02	1.15E+00±3.39E-02	1.21E+00±2.42E-02	1.28E+00±9.68E-03
GLRLM_LGRE	1.25E-02±1.18E-03	1.15E-02±1.40E-03	9.67E-03±6.56E-04	3.31E-03±3.16E-04	3.00E-03±3.72E-04	2.51E-03±1.74E-04
GLRLM_HGRE	9.70E+01±7.86E+00	1.06E+02±1.12E+01	1.22E+02±6.16E+00	3.71E+02±3.02E+01	4.07E+02±4.28E+01	4.71E+02±2.35E+01
GLRLM_SRLGE	1.17E-02±1.07E-03	1.05E-02±1.30E-03	8.73E-03±6.10E-04	3.20E-03±2.94E-04	2.87E-03±3.55E-04	2.39E-03±1.64E-04
GLRLM_SRHGE	8.90E+01±8.00E+00	9.43E+01±1.01E+01	1.06E+02±5.91E+00	3.57E+02±3.08E+01	3.85E+02±4.03E+01	4.40E+02±2.34E+01
GLRLM_LRLGE	1.64E-02±1.86E-03	1.61E-02±1.99E-03	1.47E-02±8.63E-04	3.77E-03±4.31E-04	3.56E-03±4.59E-04	3.10E-03±2.20E-04
GLRLM_LRHGE	1.33E+02±6.42E+00	1.63E+02±1.60E+01	2.10E+02±9.76E+00	4.32E+02±2.98E+01	5.04E+02±5.54E+01	6.18E+02±2.42E+01
GLRLM_GLNU	1.60E+01±2.10E+00	2.78E+01±3.69E+00	5.98E+01±2.49E+00	8.94E+00±9.92E-01	1.56E+01±2.22E+00	3.40E+01±1.53E+00
GLRLM_RLNU	8.90E+01±8.08E+00	1.61E+02±2.04E+01	3.39E+02±1.31E+01	1.04E+02±9.19E+00	1.94E+02±2.48E+01	4.24E+02±1.42E+01
GLRLM_RP	9.04E-01±7.80E-03	8.76E-01±8.29E-03	8.48E-01±4.95E-03	9.53E-01±9.38E-03	9.37E-01±6.46E-03	9.22E-01±2.53E-03
NGLDM_Coarseness	3.92E-02±8.18E-03	2.53E-02±3.79E-03	1.33E-02±7.14E-04	3.62E-02±6.68E-03	2.39E-02±3.81E-03	1.28E-02±8.47E-04
NGLDM_Contrast	1.76E-01±4.26E-02	1.49E-01±2.49E-02	1.10E-01±2.69E-02	4.00E-01±6.67E-02	3.22E-01±4.30E-02	2.37E-01±4.30E-02
NGLDM_Busyness	1.20E+00±4.93E-01	1.36E+00±2.99E-01	1.72E+00±4.95E-01	3.84E-01±1.07E-01	4.56E-01±8.66E-02	5.58E-01±1.05E-01
GLZLM_SZE	4.61E-01±6.93E-02	4.48E-01±7.48E-02	4.36E-01±5.64E-02	6.33E-01±7.21E-02	5.89E-01±4.74E-02	6.06E-01±2.81E-02
GLZLM_LZE	5.33E+01±1.81E+01	1.22E+02±4.29E+01	3.69E+02±5.39E+01	6.83E+00±2.51E+00	1.40E+01±4.86E+00	3.61E+01±6.99E+00
GLZLM_LGZE	1.36E-02±1.79E-03	1.37E-02±2.21E-03	1.23E-02±1.37E-03	3.46E-03±3.51E-04	3.29E-03±4.75E-04	2.93E-03±2.65E-04
GLZLM_HGZE	9.55E+01±1.11E+01	9.42E+01±1.53E+01	1.03E+02±1.33E+01	3.56E+02±3.16E+01	3.75E+02±5.00E+01	4.14E+02±3.10E+01
GLZLM_SZLGE	6.73E-03±9.29E-04	6.80E-03±1.85E-03	5.49E-03±1.01E-03	2.23E-03±2.41E-04	2.01E-03±3.83E-04	1.82E-03±1.55E-04
GLZLM_SZHGE	4.36E+01±1.23E+01	4.03E+01±1.13E+01	4.51E+01±8.59E+00	2.20E+02±3.35E+01	2.15E+02±2.72E+01	2.47E+02±2.82E+01
GLZLM_LZLGE	6.68E-01±2.98E-01	1.29E+00±7.33E-01	2.75E+00±4.59E-01	2.08E-02±9.05E-03	3.44E-02±1.50E-02	6.86E-02±1.54E-02
GLZLM_LZHGE	5.04E+03±1.23E+03	1.37E+04±3.37E+03	5.24E+04±6.51E+03	2.73E+03±8.96E+02	6.57E+03±1.91E+03	2.02E+04±3.34E+03
GLZLM_GLNU	3.91E+00±6.14E-01	7.08E+00±1.81E+00	1.13E+01±2.01E+00	4.84E+00±6.79E-01	7.53E+00±1.01E+00	1.37E+01±9.56E-01
GLZLM_ZLNU	5.85E+00±1.69E+00	8.64E+00±3.40E+00	1.41E+01±4.12E+00	2.33E+01±6.77E+00	3.30E+01±7.79E+00	6.46E+01±7.23E+00
GLZLM_ZP	2.15E-01±4.12E-02	1.67E-01±2.51E-02	1.28E-01±1.13E-02	5.06E-01±7.15E-02	4.15E-01±4.11E-02	3.44E-01±1.57E-02

Supplementary Table 4. Texture feature values of continuous bed motion images using fixed bin number discretization derived from observer 1.

	discrete value 64			discrete value 128		
	22 mm	28mm	37mm	22 mm	28mm	37mm
GLCM_Homogeneity	1.25E-01±6.59E-03	1.44E-01±9.46E-03	1.63E-01±4.45E-03	7.50E-02±5.59E-03	8.71E-02±6.06E-03	1.00E-01±2.40E-03
GLCM_Energy	7.22E-03±9.60E-04	3.59E-03±5.59E-04	1.82E-03±8.91E-05	6.86E-03±8.33E-04	3.22E-03±5.07E-04	1.38E-03±6.51E-05
GLCM_Contrast	4.21E+02±6.20E+01	3.14E+02±5.41E+01	2.25E+02±2.62E+01	1.68E+03±2.49E+02	1.26E+03±2.18E+02	8.98E+02±1.05E+02
GLCM_Correlation	2.36E-01±1.33E-02	3.28E-01±3.91E-02	3.85E-01±2.22E-02	2.36E-01±1.30E-02	3.28E-01±3.90E-02	3.85E-01±2.21E-02
GLCM_Entropy_log10	2.16E+00±5.66E-02	2.47E+00±6.60E-02	2.79E+00±2.00E-02	2.17E+00±5.29E-02	2.50E+00±6.68E-02	2.88E+00±1.99E-02
GLCM_Dissimilarity	1.65E+01±1.14E+00	1.40E+01±1.19E+00	1.17E+01±6.26E-01	3.30E+01±2.28E+00	2.81E+01±2.40E+00	2.35E+01±1.26E+00
GLRLM_SRE	9.90E-01±4.52E-03	9.86E-01±2.30E-03	9.82E-01±7.29E-04	9.95E-01±2.38E-03	9.94E-01±1.40E-03	9.91E-01±7.81E-04
GLRLM_LRE	1.04E+00±1.81E-02	1.06E+00±9.64E-03	1.07E+00±3.45E-03	1.02E+00±9.50E-03	1.02E+00±5.61E-03	1.04E+00±2.93E-03
GLRLM_LGRE	4.98E-02±1.28E-02	5.33E-02±7.24E-03	3.47E-02±2.79E-03	3.00E-02±8.20E-03	3.07E-02±4.82E-03	1.73E-02±4.41E-03
GLRLM_HGRE	8.39E+02±7.84E+01	8.77E+02±1.78E+02	9.24E+02±1.14E+02	3.30E+03±3.13E+02	3.46E+03±7.10E+02	3.65E+03±4.58E+02
GLRLM_SRLGE	4.94E-02±1.24E-02	5.22E-02±6.77E-03	3.44E-02±2.74E-03	2.99E-02±8.19E-03	3.04E-02±4.79E-03	1.72E-02±4.36E-03
GLRLM_SRHGE	8.31E+02±7.77E+01	8.63E+02±1.76E+02	9.05E+02±1.11E+02	3.28E+03±3.13E+02	3.44E+03±7.06E+02	3.61E+03±4.48E+02
GLRLM_LRLGE	5.13E-02±1.43E-02	5.79E-02±9.21E-03	3.58E-02±2.99E-03	3.00E-02±8.20E-03	3.19E-02±5.02E-03	1.76E-02±4.63E-03
GLRLM_LRHGE	8.70E+02±8.30E+01	9.31E+02±1.87E+02	1.01E+03±1.29E+02	3.37E+03±3.15E+02	3.56E+03±7.26E+02	3.81E+03±4.93E+02
GLRLM_GLNU	3.16E+00±1.64E-01	5.26E+00±4.92E-01	1.14E+01±4.90E-01	2.13E+00±7.84E-02	3.13E+00±2.76E-01	6.26E+00±2.02E-01
GLRLM_RLNU	1.15E+02±1.12E+01	2.23E+02±3.12E+01	5.00E+02±2.02E+01	1.17E+02±1.19E+01	2.29E+02±3.15E+01	5.17E+02±1.92E+01
GLRLM_RP	9.87E-01±5.80E-03	9.82E-01±2.97E-03	9.76E-01±1.01E-03	9.94E-01±3.10E-03	9.92E-01±1.82E-03	9.88E-01±9.63E-04
NGLDM_Coarseness	2.76E-02±4.67E-03	1.93E-02±3.28E-03	1.14E-02±9.24E-04	1.68E-02±9.76E-03	1.35E-02±7.95E-03	1.04E-02±7.52E-04
NGLDM_Contrast	1.77E+00±2.95E-01	1.42E+00±1.97E-01	9.75E-01±1.60E-01	2.91E+00±1.69E+00	2.36E+00±1.35E+00	2.12E+00±2.90E-01
NGLDM_Busyness	5.08E-02±5.19E-03	4.97E-02±6.38E-03	6.48E-02±3.86E-03	2.17E-02±1.25E-02	1.43E-02±8.30E-03	1.90E-02±9.50E-04
GLZLM_SZE	8.72E-01±5.32E-02	8.44E-01±2.31E-02	8.12E-01±6.10E-03	9.39E-01±2.76E-02	9.19E-01±2.06E-02	8.94E-01±5.82E-03
GLZLM_LZE	1.62E+00±3.43E-01	2.08E+00±2.31E-01	2.63E+00±1.56E-01	1.29E+00±1.60E-01	1.37E+00±7.90E-02	1.63E+00±7.07E-02
GLZLM_LGZE	5.15E-02±9.49E-03	4.99E-02±5.67E-03	4.05E-02±3.23E-03	3.24E-02±9.39E-03	2.88E-02±6.02E-03	1.86E-02±4.18E-03
GLZLM_HGZE	8.51E+02±9.47E+01	8.54E+02±1.62E+02	8.70E+02±9.18E+01	3.27E+03±3.61E+02	3.40E+03±6.77E+02	3.57E+03±4.08E+02
GLZLM_SZLGE	4.58E-02±5.06E-03	4.06E-02±3.53E-03	3.61E-02±3.53E-03	3.23E-02±9.35E-03	2.53E-02±6.61E-03	1.73E-02±3.48E-03
GLZLM_SZHGE	7.55E+02±9.75E+01	7.10E+02±1.38E+02	6.79E+02±7.58E+01	3.05E+03±3.93E+02	3.09E+03±6.34E+02	3.14E+03±3.23E+02
GLZLM_LZLGE	7.57E-02±3.72E-02	1.25E-01±3.54E-02	6.20E-02±7.06E-03	3.26E-02±9.57E-03	4.82E-02±1.24E-02	2.35E-02±7.39E-03
GLZLM_LZHGE	1.35E+03±3.27E+02	1.92E+03±4.01E+02	2.72E+03±4.97E+02	4.29E+03±6.30E+02	4.86E+03±9.68E+02	6.26E+03±1.10E+03
GLZLM_GLNU	2.66E+00±1.62E-01	4.11E+00±4.87E-01	8.11E+00±2.88E-01	1.96E+00±6.79E-02	2.79E+00±3.12E-01	5.15E+00±1.08E-01
GLZLM_ZLNU	7.28E+01±1.25E+01	1.24E+02±2.85E+01	2.40E+02±1.28E+01	9.37E+01±8.42E+00	1.72E+02±3.57E+01	3.47E+02±9.43E+00
GLZLM_ZP	8.44E-01±6.33E-02	7.84E-01±3.03E-02	7.30E-01±9.62E-03	9.20E-01±3.70E-02	8.97E-01±2.14E-02	8.53E-01±1.05E-02

Supplementary Table 5. Texture feature values of step-and-shoot images using fixed bin size discretization derived from observer 2.

	discrete value 64			discrete value 128		
	22 mm	28mm	37mm	22 mm	28mm	37mm
GLCM_Homogeneity	4.41E-01±8.94E-03	4.68E-01±8.26E-03	5.03E-01±3.81E-03	3.04E-01±1.01E-02	3.30E-01±5.20E-03	3.58E-01±4.81E-03
GLCM_Energy	2.53E-02±1.39E-03	2.40E-02±2.30E-03	2.76E-02±2.12E-03	1.17E-02±6.28E-04	8.67E-03±4.84E-04	8.17E-03±7.55E-04
GLCM_Contrast	6.67E+00±6.70E-01	5.78E+00±4.42E-01	4.54E+00±1.89E-01	2.61E+01±2.25E+00	2.26E+01±1.66E+00	1.78E+01±9.39E-01
GLCM_Correlation	2.63E-01±2.07E-02	3.52E-01±3.19E-02	4.18E-01±1.85E-02	2.66E-01±1.94E-02	3.54E-01±3.05E-02	4.21E-01±1.86E-02
GLCM_Entropy_log10	1.66E+00±2.24E-02	1.71E+00±3.36E-02	1.68E+00±1.97E-02	1.99E+00±2.83E-02	2.15E+00±2.09E-02	2.20E+00±2.52E-02
GLCM_Dissimilarity	2.06E+00±1.04E-01	1.88E+00±7.25E-02	1.63E+00±3.39E-02	4.12E+00±1.90E-01	3.75E+00±1.28E-01	3.27E+00±8.31E-02
GLRLM_SRE	9.19E-01±6.11E-03	9.01E-01±3.15E-03	8.77E-01±3.16E-03	9.60E-01±6.25E-03	9.48E-01±2.35E-03	9.36E-01±2.88E-03
GLRLM_LRE	1.37E+00±3.56E-02	1.51E+00±3.33E-02	1.70E+00±2.91E-02	1.17E+00±2.65E-02	1.23E+00±1.28E-02	1.31E+00±1.95E-02
GLRLM_LGRE	1.36E-02±1.51E-03	1.21E-02±7.97E-04	1.06E-02±4.28E-04	3.58E-03±4.01E-04	3.15E-03±2.10E-04	2.75E-03±1.24E-04
GLRLM_HGRE	9.01E+01±8.66E+00	1.01E+02±5.80E+00	1.13E+02±3.75E+00	3.45E+02±3.37E+01	3.91E+02±2.18E+01	4.38E+02±1.46E+01
GLRLM_SRLGE	1.27E-02±1.39E-03	1.12E-02±7.29E-04	9.54E-03±3.54E-04	3.46E-03±3.80E-04	3.02E-03±2.02E-04	2.61E-03±1.17E-04
GLRLM_SRHGE	8.18E+01±8.68E+00	8.93E+01±5.50E+00	9.68E+01±3.48E+00	3.28E+02±3.52E+01	3.67E+02±2.05E+01	4.06E+02±1.36E+01
GLRLM_LRLGE	1.80E-02±2.16E-03	1.70E-02±1.30E-03	1.65E-02±9.74E-04	4.12E-03±4.93E-04	3.74E-03±2.58E-04	3.43E-03±1.75E-04
GLRLM_LRHGE	1.29E+02±8.45E+00	1.64E+02±8.63E+00	2.08E+02±4.80E+00	4.16E+02±2.85E+01	5.01E+02±2.79E+01	5.94E+02±2.13E+01
GLRLM_GLNU	1.68E+01±1.79E+00	2.84E+01±1.94E+00	6.32E+01±2.02E+00	9.58E+00±1.26E+00	1.61E+01±1.16E+00	3.61E+01±1.06E+00
GLRLM_RLNU	9.26E+01±9.53E+00	1.68E+02±1.02E+01	3.50E+02±1.10E+01	1.08E+02±1.09E+01	2.04E+02±1.41E+01	4.45E+02±1.72E+01
GLRLM_RP	8.98E-01±7.66E-03	8.70E-01±5.85E-03	8.35E-01±4.10E-03	9.48E-01±7.57E-03	9.32E-01±3.01E-03	9.14E-01±4.33E-03
NGLDM_Coarseness	3.77E-02±5.60E-03	2.39E-02±1.43E-03	1.23E-02±6.63E-04	3.46E-02±5.09E-03	2.22E-02±1.95E-03	1.18E-02±7.15E-04
NGLDM_Contrast	1.82E-01±4.12E-02	1.62E-01±1.69E-02	1.33E-01±1.56E-02	3.86E-01±5.47E-02	3.54E-01±2.94E-02	2.67E-01±3.14E-02
NGLDM_Busyness	1.38E+00±5.18E-01	1.40E+00±1.64E-01	2.23E+00±3.91E-01	4.20E-01±5.52E-02	4.67E-01±4.97E-02	6.43E-01±1.18E-01
GLZLM_SZE	4.69E-01±8.03E-02	4.32E-01±1.03E-01	3.90E-01±7.30E-02	6.46E-01±3.52E-02	5.92E-01±2.86E-02	6.00E-01±3.77E-02
GLZLM_LZE	5.11E+01±1.20E+01	1.17E+02±3.10E+01	4.94E+02±1.02E+02	7.23E+00±1.18E+00	1.62E+01±3.40E+00	5.59E+01±1.16E+01
GLZLM_LGZE	1.55E-02±1.69E-03	1.54E-02±2.04E-03	1.37E-02±3.07E-04	3.81E-03±4.82E-04	3.60E-03±3.09E-04	3.33E-03±1.54E-04
GLZLM_HGZE	8.22E+01±1.06E+01	8.31E+01±1.07E+01	9.00E+01±4.03E+00	3.21E+02±4.17E+01	3.41E+02±2.57E+01	3.62E+02±1.18E+01
GLZLM_SZLGE	8.16E-03±1.45E-03	7.72E-03±2.38E-03	5.53E-03±1.37E-03	2.54E-03±3.63E-04	2.26E-03±2.12E-04	2.08E-03±1.21E-04
GLZLM_SZHGE	3.48E+01±1.27E+01	3.16E+01±8.59E+00	3.47E+01±4.32E+00	1.99E+02±2.78E+01	1.91E+02±2.74E+01	2.09E+02±1.62E+01
GLZLM_LZLGE	6.82E-01±1.94E-01	1.12E+00±3.50E-01	3.91E+00±1.00E+00	2.37E-02±4.69E-03	3.78E-02±7.43E-03	1.09E-01±2.22E-02
GLZLM_LZHGE	4.62E+03±9.27E+02	1.40E+04±3.03E+03	6.72E+04±1.15E+04	2.74E+03±3.86E+02	8.00E+03±1.93E+03	3.05E+04±6.28E+03
GLZLM_GLNU	4.38E+00±3.99E-01	7.34E+00±1.43E+00	1.20E+01±2.54E+00	5.31E+00±5.58E-01	8.07E+00±3.95E-01	1.40E+01±9.20E-01
GLZLM_ZLNU	6.44E+00±1.59E+00	9.03E+00±3.17E+00	1.11E+01±4.62E+00	2.49E+01±3.46E+00	3.43E+01±3.97E+00	6.13E+01±1.08E+01
GLZLM_ZP	2.16E-01±2.49E-02	1.69E-01±2.89E-02	1.11E-01±2.19E-02	4.97E-01±2.04E-02	4.06E-01±2.68E-02	3.11E-01±2.58E-02

Supplementary Table 6. Texture feature values of step-and-shoot images using fixed bin number discretization derived from observer 2.

	discrete value 64			discrete value 128		
	22 mm	28mm	37mm	22 mm	28mm	37mm
GLCM_Homogeneity	1.25E-01±5.72E-03	1.43E-01±7.28E-03	1.62E-01±4.59E-03	7.64E-02±4.25E-03	8.69E-02±5.04E-03	1.00E-01±3.08E-03
GLCM_Energy	6.71E-03±9.67E-04	3.31E-03±2.72E-04	1.69E-03±1.33E-04	6.41E-03±9.20E-04	2.96E-03±2.39E-04	1.27E-03±5.16E-05
GLCM_Contrast	4.17E+02±6.28E+01	3.37E+02±3.06E+01	2.46E+02±2.49E+01	1.67E+03±2.53E+02	1.35E+03±1.20E+02	9.84E+02±9.99E+01
GLCM_Correlation	2.67E-01±2.00E-02	3.56E-01±2.69E-02	4.24E-01±1.69E-02	2.67E-01±1.96E-02	3.56E-01±2.68E-02	4.24E-01±1.68E-02
GLCM_Entropy_log10	2.19E+00±6.09E-02	2.50E+00±3.40E-02	2.82E+00±2.74E-02	2.20E+00±6.04E-02	2.54E+00±3.45E-02	2.91E+00±1.71E-02
GLCM_Dissimilarity	1.65E+01±1.30E+00	1.45E+01±6.58E-01	1.22E+01±5.99E-01	3.30E+01±2.61E+00	2.90E+01±1.29E+00	2.44E+01±1.21E+00
GLRLM_SRE	9.89E-01±2.03E-03	9.86E-01±2.11E-03	9.82E-01±8.24E-04	9.94E-01±9.81E-04	9.94E-01±1.33E-03	9.91E-01±8.09E-04
GLRLM_LRE	1.04E+00±7.29E-03	1.06E+00±9.14E-03	1.08E+00±3.26E-03	1.02E+00±3.92E-03	1.03E+00±6.26E-03	1.04E+00±3.01E-03
GLRLM_LGRE	5.00E-02±1.29E-02	4.65E-02±1.28E-02	3.04E-02±9.74E-03	2.79E-02±9.13E-03	2.68E-02±7.60E-03	1.53E-02±6.33E-03
GLRLM_HGRE	8.65E+02±1.56E+02	1.03E+03±1.63E+02	1.11E+03±9.92E+01	3.42E+03±6.26E+02	4.06E+03±6.53E+02	4.38E+03±3.97E+02
GLRLM_SRLGE	4.98E-02±1.28E-02	4.61E-02±1.24E-02	3.02E-02±9.60E-03	2.79E-02±9.11E-03	2.67E-02±7.60E-03	1.52E-02±6.27E-03
GLRLM_SRHGE	8.51E+02±1.53E+02	1.01E+03±1.63E+02	1.08E+03±9.66E+01	3.39E+03±6.21E+02	4.03E+03±6.57E+02	4.33E+03±3.93E+02
GLRLM_LRLGE	5.08E-02±1.34E-02	4.83E-02±1.42E-02	3.15E-02±1.03E-02	2.80E-02±9.21E-03	2.68E-02±7.60E-03	1.55E-02±6.55E-03
GLRLM_LRHGE	9.24E+02±1.71E+02	1.11E+03±1.64E+02	1.22E+03±1.09E+02	3.55E+03±6.43E+02	4.20E+03±6.38E+02	4.60E+03±4.14E+02
GLRLM_GLNU	3.15E+00±1.48E-01	5.20E+00±2.06E-01	1.14E+01±4.97E-01	2.05E+00±5.35E-02	3.06E+00±1.27E-01	6.23E+00±2.88E-01
GLRLM_RLNU	1.21E+02±1.39E+01	2.37E+02±1.76E+01	5.35E+02±1.71E+01	1.24E+02±1.44E+01	2.44E+02±1.71E+01	5.55E+02±1.73E+01
GLRLM_RP	9.86E-01±2.46E-03	9.81E-01±2.84E-03	9.76E-01±9.98E-04	9.93E-01±1.27E-03	9.92E-01±1.91E-03	9.88E-01±1.00E-03
NGLDM_Coarseness	2.70E-02±3.76E-03	1.83E-02±1.24E-03	1.07E-02±4.70E-04	2.09E-02±2.28E-03	1.59E-02±9.27E-04	9.90E-03±6.77E-04
NGLDM_Contrast	1.88E+00±1.85E-01	1.59E+00±1.38E-01	1.13E+00±1.42E-01	3.81E+00±4.07E-01	3.33E+00±2.08E-01	2.43E+00±2.25E-01
NGLDM_Busyness	4.53E-02±7.13E-03	4.30E-02±8.70E-03	6.00E-02±6.58E-03	2.43E-02±4.17E-03	1.44E-02±2.60E-03	1.69E-02±2.02E-03
GLZLM_SZE	8.77E-01±2.08E-02	8.55E-01±7.98E-03	8.20E-01±1.56E-02	9.39E-01±7.29E-03	9.28E-01±1.73E-02	8.93E-01±9.53E-03
GLZLM_LZE	1.71E+00±7.23E-02	2.10E+00±2.40E-01	2.83E+00±2.09E-01	1.33E+00±6.06E-02	1.39E+00±1.21E-01	1.65E+00±7.35E-02
GLZLM_LGZE	5.51E-02±1.28E-02	4.97E-02±1.04E-02	3.58E-02±1.09E-02	3.00E-02±9.76E-03	2.94E-02±8.75E-03	1.68E-02±6.55E-03
GLZLM_HGZE	8.00E+02±1.40E+02	9.46E+02±1.60E+02	1.00E+03±9.21E+01	3.27E+03±6.05E+02	3.92E+03±7.15E+02	4.15E+03±3.97E+02
GLZLM_SZLGE	5.22E-02±1.17E-02	4.33E-02±6.43E-03	3.26E-02±9.85E-03	2.96E-02±9.48E-03	2.93E-02±8.75E-03	1.61E-02±5.97E-03
GLZLM_SZHGE	6.57E+02±1.04E+02	7.71E+02±1.37E+02	7.74E+02±7.19E+01	2.98E+03±5.70E+02	3.53E+03±7.11E+02	3.56E+03±3.64E+02
GLZLM_LZLGE	6.90E-02±2.23E-02	7.99E-02±3.66E-02	5.70E-02±2.51E-02	3.15E-02±1.09E-02	3.01E-02±8.72E-03	2.04E-02±1.04E-02
GLZLM_LZHGE	1.72E+03±3.66E+02	2.51E+03±1.37E+02	3.79E+03±4.24E+02	5.06E+03±7.69E+02	6.09E+03±4.82E+02	8.00E+03±8.55E+02
GLZLM_GLNU	2.65E+00±2.19E-01	4.14E+00±1.90E-01	8.14E+00±2.81E-01	1.83E+00±6.05E-02	2.75E+00±1.24E-01	5.18E+00±2.96E-01
GLZLM_ZLNU	7.69E+01±9.81E+00	1.36E+02±1.27E+01	2.62E+02±1.34E+01	9.88E+01±1.35E+01	1.87E+02±1.96E+01	3.71E+02±1.68E+01
GLZLM_ZP	8.35E-01±1.72E-02	7.88E-01±2.00E-02	7.25E-01±9.69E-03	9.12E-01±1.23E-02	8.99E-01±2.27E-02	8.52E-01±1.21E-02

Supplementary Table 7. Texture feature values of continuous bed motion images using fixed bin size discretization derived from observer 2.

	discrete value 64			discrete value 128		
	22 mm	28mm	37mm	22 mm	28mm	37mm
GLCM_Homogeneity	4.33E-01±8.83E-03	4.64E-01±7.08E-03	4.91E-01±7.65E-03	2.96E-01±7.58E-03	3.24E-01±6.67E-03	3.48E-01±5.79E-03
GLCM_Energy	2.55E-02±2.27E-03	2.37E-02±1.14E-03	2.59E-02±1.48E-03	1.18E-02±9.16E-04	8.61E-03±6.95E-04	7.74E-03±3.61E-04
GLCM_Contrast	7.21E+00±7.17E-01	5.85E+00±4.08E-01	4.80E+00±3.77E-01	2.86E+01±3.18E+00	2.28E+01±1.57E+00	1.87E+01±1.37E+00
GLCM_Correlation	2.29E-01±1.96E-02	3.26E-01±3.78E-02	3.75E-01±2.61E-02	2.33E-01±1.31E-02	3.29E-01±3.73E-02	3.84E-01±2.32E-02
GLCM_Entropy_log10	1.67E+00±3.68E-02	1.71E+00±2.69E-02	1.70E+00±2.95E-02	1.98E+00±3.30E-02	2.14E+00±3.64E-02	2.22E+00±2.06E-02
GLCM_Dissimilarity	2.13E+00±1.01E-01	1.89E+00±6.04E-02	1.69E+00±6.44E-02	4.29E+00±2.18E-01	3.78E+00±1.15E-01	3.38E+00±1.17E-01
GLRLM_SRE	9.24E-01±5.89E-03	9.04E-01±6.57E-03	8.85E-01±4.37E-03	9.64E-01±7.28E-03	9.52E-01±4.93E-03	9.41E-01±1.96E-03
GLRLM_LRE	1.35E+00±3.41E-02	1.48E+00±3.92E-02	1.63E+00±2.51E-02	1.15E+00±3.39E-02	1.22E+00±2.40E-02	1.28E+00±9.68E-03
GLRLM_LGRE	1.25E-02±1.18E-03	1.15E-02±1.40E-03	9.67E-03±6.56E-04	3.31E-03±3.16E-04	3.00E-03±3.71E-04	2.51E-03±1.74E-04
GLRLM_HGRE	9.70E+01±7.86E+00	1.06E+02±1.12E+01	1.22E+02±6.16E+00	3.71E+02±3.02E+01	4.07E+02±4.28E+01	4.71E+02±2.35E+01
GLRLM_SRLGE	1.17E-02±1.07E-03	1.06E-02±1.30E-03	8.73E-03±6.10E-04	3.20E-03±2.94E-04	2.88E-03±3.55E-04	2.39E-03±1.64E-04
GLRLM_SRHGE	8.90E+01±8.00E+00	9.43E+01±1.01E+01	1.06E+02±5.91E+00	3.57E+02±3.08E+01	3.85E+02±4.02E+01	4.40E+02±2.34E+01
GLRLM_LRLGE	1.64E-02±1.86E-03	1.61E-02±1.98E-03	1.47E-02±8.63E-04	3.77E-03±4.31E-04	3.57E-03±4.57E-04	3.10E-03±2.20E-04
GLRLM_LRHGE	1.33E+02±6.42E+00	1.63E+02±1.61E+01	2.10E+02±9.76E+00	4.32E+02±2.98E+01	5.04E+02±5.55E+01	6.18E+02±2.42E+01
GLRLM_GLNU	1.60E+01±2.10E+00	2.78E+01±3.68E+00	5.98E+01±2.49E+00	8.94E+00±9.92E-01	1.57E+01±2.20E+00	3.40E+01±1.53E+00
GLRLM_RLNU	8.90E+01±8.08E+00	1.61E+02±2.05E+01	3.39E+02±1.31E+01	1.04E+02±9.19E+00	1.95E+02±2.49E+01	4.24E+02±1.42E+01
GLRLM_RP	9.04E-01±7.80E-03	8.76E-01±8.17E-03	8.48E-01±4.95E-03	9.53E-01±9.38E-03	9.37E-01±6.41E-03	9.22E-01±2.53E-03
NGLDM_Coarseness	3.92E-02±8.18E-03	2.53E-02±3.76E-03	1.33E-02±7.14E-04	3.62E-02±6.68E-03	2.38E-02±3.76E-03	1.28E-02±8.47E-04
NGLDM_Contrast	1.76E-01±4.26E-02	1.49E-01±2.49E-02	1.10E-01±2.69E-02	4.00E-01±6.67E-02	3.22E-01±4.31E-02	2.37E-01±4.30E-02
NGLDM_Busyness	1.20E+00±4.93E-01	1.36E+00±2.96E-01	1.72E+00±4.95E-01	3.84E-01±1.07E-01	4.58E-01±8.44E-02	5.58E-01±1.05E-01
GLZLM_SZE	4.61E-01±6.93E-02	4.48E-01±7.48E-02	4.36E-01±5.64E-02	6.33E-01±7.21E-02	5.89E-01±4.72E-02	6.06E-01±2.81E-02
GLZLM_LZE	5.33E+01±1.81E+01	1.22E+02±4.27E+01	3.69E+02±5.39E+01	6.83E+00±2.51E+00	1.40E+01±4.83E+00	3.61E+01±6.99E+00
GLZLM_LGZE	1.36E-02±1.79E-03	1.37E-02±2.21E-03	1.23E-02±1.37E-03	3.46E-03±3.51E-04	3.29E-03±4.73E-04	2.93E-03±2.65E-04
GLZLM_HGZE	9.55E+01±1.11E+01	9.42E+01±1.53E+01	1.03E+02±1.33E+01	3.56E+02±3.16E+01	3.73E+02±5.15E+01	4.14E+02±3.10E+01
GLZLM_SZLGE	6.73E-03±9.29E-04	6.80E-03±1.85E-03	5.49E-03±1.01E-03	2.23E-03±2.41E-04	2.01E-03±3.83E-04	1.82E-03±1.55E-04
GLZLM_SZHGE	4.36E+01±1.23E+01	4.03E+01±1.13E+01	4.51E+01±8.59E+00	2.20E+02±3.35E+01	2.15E+02±2.74E+01	2.47E+02±2.82E+01
GLZLM_LZLGE	6.68E-01±2.98E-01	1.29E+00±7.30E-01	2.75E+00±4.59E-01	2.08E-02±9.05E-03	3.46E-02±1.49E-02	6.86E-02±1.54E-02
GLZLM_LZHGE	5.04E+03±1.23E+03	1.37E+04±3.35E+03	5.24E+04±6.51E+03	2.73E+03±8.96E+02	6.56E+03±1.90E+03	2.02E+04±3.34E+03
GLZLM_GLNU	3.91E+00±6.14E-01	7.08E+00±1.81E+00	1.13E+01±2.01E+00	4.84E+00±6.79E-01	7.52E+00±1.01E+00	1.37E+01±9.56E-01
GLZLM_ZLNU	5.85E+00±1.69E+00	8.62E+00±3.39E+00	1.41E+01±4.12E+00	2.33E+01±6.77E+00	3.30E+01±7.76E+00	6.46E+01±7.23E+00
GLZLM_ZP	2.15E-01±4.12E-02	1.67E-01±2.49E-02	1.28E-01±1.13E-02	5.06E-01±7.15E-02	4.15E-01±4.01E-02	3.44E-01±1.57E-02

Supplementary Table 8. Texture feature values of continuous bed motion images using fixed bin number discretization derived from observer 2.

	discrete value 64			discrete value 128		
	22 mm	28mm	37mm	22 mm	28mm	37mm
GLCM_Homogeneity	1.25E-01±6.53E-03	1.44E-01±9.36E-03	1.63E-01±4.45E-03	7.49E-02±5.42E-03	8.72E-02±6.01E-03	1.00E-01±2.40E-03
GLCM_Energy	7.22E-03±9.68E-04	3.59E-03±5.59E-04	1.82E-03±8.91E-05	6.85E-03±8.45E-04	3.22E-03±5.07E-04	1.38E-03±6.51E-05
GLCM_Contrast	4.20E+02±6.15E+01	3.14E+02±5.42E+01	2.25E+02±2.62E+01	1.68E+03±2.46E+02	1.26E+03±2.18E+02	8.98E+02±1.05E+02
GLCM_Correlation	2.36E-01±1.33E-02	3.29E-01±3.94E-02	3.85E-01±2.22E-02	2.36E-01±1.31E-02	3.29E-01±3.93E-02	3.85E-01±2.21E-02
GLCM_Entropy_log10	2.16E+00±5.67E-02	2.47E+00±6.60E-02	2.79E+00±2.00E-02	2.17E+00±5.36E-02	2.50E+00±6.68E-02	2.88E+00±1.99E-02
GLCM_Dissimilarity	1.65E+01±1.13E+00	1.40E+01±1.19E+00	1.17E+01±6.26E-01	3.30E+01±2.26E+00	2.81E+01±2.40E+00	2.35E+01±1.26E+00
GLRLM_SRE	9.90E-01±4.35E-03	9.86E-01±2.29E-03	9.82E-01±7.29E-04	9.95E-01±1.93E-03	9.94E-01±1.40E-03	9.91E-01±7.81E-04
GLRLM_LRE	1.04E+00±1.74E-02	1.06E+00±9.60E-03	1.07E+00±3.45E-03	1.02E+00±7.71E-03	1.02E+00±5.58E-03	1.04E+00±2.93E-03
GLRLM_LGRE	4.86E-02±1.12E-02	5.35E-02±6.99E-03	3.47E-02±2.79E-03	2.96E-02±7.79E-03	3.07E-02±4.80E-03	1.73E-02±4.41E-03
GLRLM_HGRE	8.39E+02±7.88E+01	8.75E+02±1.78E+02	9.24E+02±1.14E+02	3.30E+03±3.15E+02	3.45E+03±7.10E+02	3.65E+03±4.58E+02
GLRLM_SRLGE	4.83E-02±1.09E-02	5.23E-02±6.51E-03	3.44E-02±2.74E-03	2.96E-02±7.79E-03	3.04E-02±4.77E-03	1.72E-02±4.36E-03
GLRLM_SRHGE	8.31E+02±7.80E+01	8.62E+02±1.76E+02	9.05E+02±1.11E+02	3.28E+03±3.15E+02	3.43E+03±7.06E+02	3.61E+03±4.48E+02
GLRLM_LRLGE	5.01E-02±1.27E-02	5.81E-02±8.95E-03	3.58E-02±2.99E-03	2.97E-02±7.80E-03	3.19E-02±5.01E-03	1.76E-02±4.63E-03
GLRLM_LRHGE	8.71E+02±8.41E+01	9.29E+02±1.87E+02	1.01E+03±1.29E+02	3.37E+03±3.15E+02	3.55E+03±7.26E+02	3.81E+03±4.93E+02
GLRLM_GLNU	3.12E+00±9.74E-02	5.26E+00±4.89E-01	1.14E+01±4.90E-01	2.10E+00±4.97E-02	3.14E+00±2.76E-01	6.26E+00±2.02E-01
GLRLM_RLNU	1.15E+02±1.13E+01	2.23E+02±3.12E+01	5.00E+02±2.02E+01	1.17E+02±1.22E+01	2.30E+02±3.15E+01	5.17E+02±1.92E+01
GLRLM_RP	9.88E-01±5.58E-03	9.82E-01±2.96E-03	9.76E-01±1.01E-03	9.94E-01±2.51E-03	9.92E-01±1.81E-03	9.88E-01±9.63E-04
NGLDM_Coarseness	2.80E-02±4.19E-03	1.93E-02±3.28E-03	1.14E-02±9.24E-04	1.71E-02±9.79E-03	1.35E-02±7.95E-03	1.04E-02±7.52E-04
NGLDM_Contrast	1.77E+00±2.92E-01	1.42E+00±1.98E-01	9.75E-01±1.60E-01	2.91E+00±1.69E+00	2.36E+00±1.35E+00	2.12E+00±2.90E-01
NGLDM_Busyness	5.01E-02±4.14E-03	4.98E-02±6.22E-03	6.48E-02±3.86E-03	2.09E-02±1.20E-02	1.44E-02±8.30E-03	1.90E-02±9.50E-04
GLZLM_SZE	8.72E-01±5.32E-02	8.44E-01±2.31E-02	8.11E-01±7.42E-03	9.44E-01±2.03E-02	9.19E-01±2.06E-02	8.95E-01±5.95E-03
GLZLM_LZE	1.62E+00±3.43E-01	2.09E+00±2.28E-01	2.63E+00±1.54E-01	1.27E+00±1.26E-01	1.37E+00±7.85E-02	1.63E+00±7.03E-02
GLZLM_LGZE	5.01E-02±7.41E-03	5.02E-02±5.34E-03	4.05E-02±3.23E-03	3.18E-02±8.57E-03	2.88E-02±5.97E-03	1.86E-02±4.18E-03
GLZLM_HGZE	8.49E+02±9.22E+01	8.53E+02±1.62E+02	8.68E+02±8.97E+01	3.27E+03±3.53E+02	3.40E+03±6.76E+02	3.57E+03±4.06E+02
GLZLM_SZLGE	4.43E-02±5.52E-03	4.08E-02±3.20E-03	3.61E-02±3.53E-03	3.18E-02±8.54E-03	2.53E-02±6.54E-03	1.73E-02±3.48E-03
GLZLM_SZHGE	7.51E+02±9.49E+01	7.09E+02±1.37E+02	6.77E+02±7.35E+01	3.05E+03±3.94E+02	3.08E+03±6.34E+02	3.15E+03±3.21E+02
GLZLM_LZLGE	7.41E-02±3.43E-02	1.26E-01±3.50E-02	6.20E-02±7.06E-03	3.20E-02±8.68E-03	4.82E-02±1.24E-02	2.35E-02±7.39E-03
GLZLM_LZHGE	1.35E+03±3.40E+02	1.92E+03±4.02E+02	2.72E+03±4.96E+02	4.25E+03±5.45E+02	4.85E+03±9.66E+02	6.27E+03±1.09E+03
GLZLM_GLNU	2.64E+00±1.89E-01	4.12E+00±4.87E-01	8.10E+00±2.90E-01	1.95E+00±7.52E-02	2.79E+00±3.12E-01	5.15E+00±1.06E-01
GLZLM_ZLNU	7.28E+01±1.25E+01	1.24E+02±2.85E+01	2.40E+02±1.29E+01	9.52E+01±8.67E+00	1.72E+02±3.56E+01	3.48E+02±9.06E+00
GLZLM_ZP	8.44E-01±6.33E-02	7.83E-01±3.00E-02	7.31E-01±8.76E-03	9.24E-01±2.91E-02	8.97E-01±2.14E-02	8.53E-01±1.02E-02